

Frequency-domain View on Financial Cycles: Empirical Evidence from Europe

A thesis presented for the degree of

Master of Science (M.Sc.)

in

Quantitative Finance

at

Graduate School of Economics, Finance, and Management

Johan Wolfgang Goethe-Universität Frankfurt am Main



Ville Voutilainen

April 24, 2017

Supervisor:

Prof. Dr. Uwe Hassler

Statistics and Econometric Methods

Faculty of Economics and Business Administration

Johan Wolfgang Goethe-Universität Frankfurt am Main

Abstract

In this thesis we construct a composite indicator for the financial cycle in the spirit of Schüler et al. (2015). The analysis relies on selecting most relevant co-movement in several key macro-financial variables using spectral methods. To this end, a detailed description of the needed frequency-domain theory is presented. We show that the obtained financial cycle proxy makes a useful addition to the macroprudential toolkit as it succeeds well in early identification of financial stress.

Acknowledgements

I was fortunate enough to receive a lot of support during my struggles to complete this thesis. First and foremost I want to thank Bank of Finland for the opportunity to write my thesis while working in the Macroprudential Analysis Division. I thank my boss Paavo Miettinen for allowing me to conduct independent research. I would also like to express my gratitude to my colleagues for their assistance, especially to Eero Tölö who was always ready to discuss questions on theory and technical implementation. Furthermore, I want to thank my mother Sari, father Esa, and brother Kalle for their love and support throughout the years. A special thanks to Sari Nissinen for believing in me and putting up with my quirks. And last but not least, I want to thank a very special group of people who I suffered with during the hardest times of our graduate studies. Without you I never would have graduated.

Contents

Glossary	5
List of Symbols	6
List of Figures	7
List of Tables	8
1 Introduction	9
1.1 Motivation for financial cycles	9
1.2 Practicalities regarding the thesis	10
2 Theory of Spectral Analysis	12
2.1 Motivation for frequency-domain analysis	12
2.2 Fourier analysis	13
2.2.1 Fourier transform and Parseval's relation	14
2.2.2 Family portrait of discrete-time Fourier transforms	18
2.3 Spectral analysis of stationary processes	22
2.3.1 Univariate spectrum	22
2.3.2 Cross-spectrum	24
2.4 Estimation of spectral densities	25
2.4.1 Univariate natural estimators	25
2.4.2 Consistent estimation of univariate spectrum	27
2.4.3 Multivariate estimators	30
3 Constructing Composite Financial Cycle	32
3.1 Selecting relevant variables	32
3.2 Stress index	34
3.2.1 Pre-multiplying variables	35
3.2.2 Normalizing variables	36
3.2.3 Aggregation of variables	38

CONTENTS

3.3	Power Cohesion and endogenous frequency band	39
3.4	Filtering the stress index	41
4	Empirical Results	43
4.1	Visualization of Composite Financial Cycles	43
4.2	Early warning properties	47
4.2.1	Pooled logit early warning regression	47
4.2.2	Comparison of CFC and Financial Stress Index for Finland	52
4.3	Comparing results with Schüler et al. (2015)	54
5	Conclusion	56
	Appendix A	57
A.1	Circular shift	57
A.2	Raw series	58
A.3	Deflating nominal raw series	58
A.4	De-trending series	59
A.5	Random Walk filter	64
A.6	Matlab code for Blacmman-Tukey spectral density estimator	65
A.7	Power Cohesions	71
A.8	Crisis Database	72

Glossary

Bond yield	Short-hand for government benchmark 10-year bond yield.
CFC	Composite Financial Cycle.
Credit	Short-hand for credit to private sector.
DFT	Discrete Fourier Transform.
DTFT	Discrete Time Fourier Transform. See also FFT.
ECDF	Empirical Cumulative Distribution Function.
EWMA	Exponentially Weighted Moving Average.
FFT	Finite Fourier Transform.
Financial cycle variables	Group of variables used to construct CFC.
FSI	Financial Stress Index as in Huotari (2015).
House prices	Short-hand for residential property prices.
PCoh	Power Cohesion, metric introduced in Schüler et al. (2015).
Raw series	Variable time series before any transformations.
Signal	In this thesis, a finite sample extracted from a time series.
Stocks	Short-hand for stock market index.

List of Symbols

η_X	Discrete Fourier transformation of X .
f	Frequency, cycles per unit time.
$G(\omega)$	Fourier transform of $X(t)$.
$\gamma(r)$	Autocovariance function.
$h(\omega)$	Power spectral density function.
ν_X	Discrete-time Fourier transform of X .
ω	Angular frequency, rotation in radians.
ψ	Stress index, obtained by aggregation of stress factors.
X	Arbitrary vector of values.
$X(t)$	Arbitrary real-valued function.
ξ_X	Finite Fourier transform of X .
\bar{X}	Ordered sample, values of vector X in ascending order.
$X^{[-m]}$	Circularly shifted (m steps to the right) version of vector X .
$\{X\}_t$	Arbitrary time series.
$\{z\}_t$	ECDF-transformed version of series $\{X\}_t$.

List of Figures

2.1	Parzen lag window with truncation parameter $M = 69$	30
3.1	Roadmap to Chapter 3.	33
4.1	Composite Financial Cycles for sample countries.	44
4.2	Range of deviations of CFCs from their historical mean values.	46
4.3	Comparison of the FSI and the CFC.	53
A.1	Power Cohesions for individual countries.	71

List of Tables

2.1	How increasing/decreasing M affects properties of $\hat{h}(\omega)^{BT}$	30
3.1	Financial cycle variables used in constructing Composite Financial Cycles.	34
3.2	Common time samples of financial cycle variables.	35
4.1	Ranges of identified periodicity bands measured in years.	47
4.2	Confusion matrix.	49
4.3	Early warning regression results.	51
A.1	Raw series credit.	60
A.2	Raw series house prices.	61
A.3	Raw series stocks.	62
A.4	Raw series bond yield.	63
A.5	Crisis periods for the sample countries in Laeven and Valencia (2012) banking crisis data set.	72

Chapter 1

Introduction

1.1 Motivation for financial cycles

The study of business cycles is in the core of macroeconomic research. This comes as no big surprise as the so called boom-and-bust cycles are important for the functionality of economies. Further, cyclical nature of economy is an interesting academic topic by its own right. Contrary to its well-know cousin, *financial cycle* is a less familiar phenomenon. This might seem surprising as the study of financial cycles actually pre-dates that of business cycles (Borio, 2014, p. 182). However, financial cycles fell out of favour during the post-war period, not the least due to paradigms such as the Modigliani-Miller theorem and real business-cycle theory, which emphasized the real side side of the economy over nominal quantities. It wasn't until the financial crisis of 2007-2008 that sparked interest in financial cycles again. At this point it became clear that academics and policy makers alike had overlooked the interconnectedness of financial markets and real side of the economy, which led to hard felt – and in particular, *real* – consequences.

What are financial cycles then? Unfortunately, there exists no commonly agreed upon definition. However, most often the term "financial cycle" refers to a notion capturing the extent of imbalances in macro-financial sector. One often quoted definition is due to Borio (2014), according to whom financial cycles can be thought to reflect "self-reinforcing interactions between perceptions of value and risk, attitudes towards risk and financing constraints, which translate into booms followed by busts." This definition encompasses the analytical properties of a financial cycle but is as such hard to grasp in practical terms. In practice, a common approach is to scrutinize cyclical properties of a set of key macro-financial variables. The essential question is thus which variables should one include in the analysis.

Perhaps the most used variable in research revolving around financial cyclicalities is credit. Indeed, works by Aikman et al. (2015), Schularick and Taylor (2012), and

Geanakolpos (2010) have stressed the role of credit in determining swings in financial conditions and asset prices. This view has not gone unnoticed in policy work either, as the credit-to-GDP gap is firmly baked into the influential Basel accords. A closely related stance is to look at the co-movement of credit and housing prices. This is exactly the approach adopted in Drehmann et al. (2012) who find that credit and housing prices exhibit important common medium-term fluctuations. Furthermore, authors find that peaks in the swings of these variables are closely associated with onsets of financial/banking crises. Claessens et al. (2011) provide further insight that cycles in credit and housing prices tend to be long and severe.

In addition to credit and housing prices, also equity and other asset prices have been considered as additional building blocks of financial cycles. The results are mixed. Drehmann et al. (2012) find equity prices to be less important by claiming that they don't exhibit considerable medium-term co-movement with credit and housing prices. This stance has been recently challenged by Schüler et al. (2015) who argue that stock prices do share relevant co-movement with credit and housing prices, but bond yields less so.

Summarizing the above discussion, financial cycles exhibit following stylized facts:

1. In its most parsimonious form, financial cycles can be thought of as changes in credit and property prices. Relevancy of asset prices is less clear.
2. Financial cycles have generally rather long periods, exceeding those of business cycles.
3. Peaks in financial cycles are associated with financial crises.

From these stylized facts we can deduce that it is worthwhile to know the current phase of the financial cycle for two reasons in particular. First, understanding cyclicalities exceeding those of usual business cycle fluctuations would offer a more robust view on current economic developments. Second, it may offer an approach for early detection of costly financial crises, which is of great interest to many parties, not the least to market regulators.

1.2 Practicalities regarding the thesis

The motivation for this thesis arose from a practical vein. At the time of writing I was working at the Macroprudential Analysis Division of Bank of Finland, and my department was interested in a tool with which one could proxy the current phase of the financial cycle. In this thesis we will go through a detailed construction of a proxy for the financial cycle, which we call the *Composite Financial Cycle*, or CFC for short. The methodology

follows that of a research piece *Characterising the financial cycle: a multivariate and time-varying approach* by Yves Schüler, Paul Hiebert, and Tuomas Peltonen (Schüler et al., 2015). The CFC sums information from several key macro-financial variables in a multivariate fashion. Further, it is by construction a parsimonious measure that includes only the most relevant co-movement in selected variables.

The thesis is empirical in nature. This means that proofs and technical details are mostly left out. In return we build more on intuition when presenting theory and results. In the theoretical part of the thesis we use two types of elements to present the most important concepts:

- **Results** are important theorems/outcomes/results introduced in source texts. They are not formally proven, but the underlying reasoning is presented in the narrative leading to them. Reader is pointed to the corresponding pages in reference text.
- **Definitions** summarize important concept definitions. Often they are modified slightly to match the notation and conventions used in this thesis. As with Results, reader is pointed to the corresponding pages in reference text.

The contributions of my thesis are a) double-checking key results presented in Schüler et al. (2015), b) a more thorough treatment of the technical issues behind the construction of the CFC than in the original paper, c) a more detailed empirical examination for Finland how well the CFC can predict periods of financial stress, and finally d) providing a ready-made tool to be used in further policy analysis at Bank of Finland.

The rest of the thesis is organized as follows. In Chapter 2 we introduce theory of spectral analysis essential for the construction of the CFC. Chapter 3 treats the construction of the CFC. In Chapter 4 we present our empirical findings for the phase of the CFC as well as its early warning properties. Finally, Chapter 5 concludes.

Chapter 2

Theory of Spectral Analysis

This chapter covers the needed theoretical aspects for constructing our proxy of the financial cycle. First, we motivate the need for frequency-domain analysis. Second, reader is introduced to the single-most important tool in frequency-domain analysis, namely the Fourier transform. Third, the link between Fourier transform and spectral analysis is built. Lastly, we discuss estimation of power spectral density. The exposition in this chapter relies mostly on the excellent book series *Spectral Analysis and Time Series* by M.B. Priestley (Priestley, 1981a and Priestley, 1981b), but also on a slightly more practical oriented book by Stoica and Moses (2004) as well as some online references.

2.1 Motivation for frequency-domain analysis

Practitioners of economics are well familiar with econometric analysis taking place in time-domain. In contrast, analysis in frequency-domain has been left to less attention. In fields such as physics and engineering frequency-domain analysis is often *the* predominant way to characterize properties of a time series. This is due to the fact that tackling a given problem in frequency-domain often lends itself to mathematical convenience, but also due to its ability to offer a different perspective to the problem. Time-domain and frequency-domain analyses can be seen as two sides of the same coin. Both provide insights into properties and dynamics of a time series, but whereas time-domain analysis focuses on how a time series evolves over time, frequency-domain analysis inspects over which range of frequencies (or equivalently, over which range of periods) the time series operates.

For an intuitive example how a different perspective can be useful, consider a pulse of light that travels through substance. In time-domain we could measure the propagation of the waveform over time. Although this might be what we are interested in, it does not explain too much about the characteristics of the pulse. Imagine now that we let the pulse run through a prism, which breaks it into a spectrum of pulses, each operating at certain

frequency (or equivalently, at certain wave length) and thus having a distinct colour. The prism effectively acts as a link between time and frequency domains, revealing all the colors that were "hidden" within the original light pulse. Indeed, it was the change of perspective to frequency-domain that revealed patterns not detectable when inspecting the pulse through time-domain analysis.

Applications of frequency-domain analysis are vast. For example, in signal processing it can be used in creating earmuffs that filter out sounds operating at certain frequencies. In medicine frequency-domain analysis allows the tools for pacemakers. Seismologist might use frequency-domain analysis to detect build-ups of high-frequency quakes. It turns out that frequency domain analysis can be a useful tool for economics and finance, too. An Economist might be interested in developments of certain economic variables. As most series are inherently noisy, a possible way to approach could be first to inspect the frequency-domain side of the coin, infer at which frequencies the most important drivers of variables lie, and then filter out the less relevant frequencies from the time series. This potentially allows to draw more coherent conclusions about the state of the economy.

2.2 Fourier analysis

In this section we start building the needed toolbox by introducing basic concepts of Fourier analysis, which construct the backbone of frequency-domain analysis. The basic idea is simple but all the more remarkable: under certain conditions we can decompose any function (or process) into a sum of sinusoids, i.e. sine and cosine functions. The rigorous formulation of this amazing result wasn't straightforward. As the name suggests, the invention of Fourier analysis has been credited to French mathematician Jean-Baptiste Joseph Fourier, who in year 1807 introduced the so-called *Fourier series* in a manuscript dealing with propagation of heat (Dominguez, 2016).

Strictly speaking, Fourier was not the first one to use Fourier series. Similar constructions were known to other great mathematician, such as Lagrange and Euler, prior to Fourier's work. However, Fourier was the first one to use Fourier series to model *arbitrary* functions. Fourier's initial work was criticized for lacking mathematical rigour and it only dealt with series of known periodicity. The refinement of the Fourier analysis took many more years and also involved other great mathematicians of the time.

2.2.1 Fourier transform and Parseval's relation

We will start by formally introducing Fourier series:

Result 2.2.1 *Fourier series*

Priestley (1981a, p. 186-189)

Let $X(t)$ be a real-valued, deterministic, and absolutely integrable function with period 2π , i.e. $X(t) = X(t + 2n)$, $n = \pm 1, \pm 2, \dots$, fulfilling some regularity conditions.¹ Then $\forall t$ we have

$$X(t) = \frac{1}{2}a_0 + \sum_{n=1}^{\infty} (a_n \cos(nt) + b_n \sin(bt)) \quad , \quad (2.1)$$

where the right-hand side is called a *Fourier series*, and a_n and b_n are called *Fourier coefficients* which are given by

$$a_n = \frac{1}{\pi} \int_{-\pi}^{\pi} X(t) \cos(nt) dt \quad (2.2)$$

$$b_n = \frac{1}{\pi} \int_{-\pi}^{\pi} X(t) \sin(nt) dt \quad (2.3)$$

for $n = 0, 1, 2, \dots$.

Fourier's initial work was criticized about not formally showing that the right-hand-side of (2.1) actually converges to function $X(t)$ (Cajori, 1894, p. 283).² Furthermore, it is not possible to apply Fourier series decomposition to non-periodic functions. In order to deal with non-periodic functions one needs an extension to the idea of Fourier series which had still been unknown to Fourier in year 1807. This extension goes by the name *Fourier integrals*. Intuitively, non-periodic functions can be thought as functions with infinite period. Using this reasoning we "might attempt to approximate a non-periodic function by a sequence of periodic functions with longer and longer periods" (Priestley, 1981a, p. 4). It turns out that – again under the same contingencies of absolute integrability and certain regularity conditions as in Result 2.2.1 – we can formalize the concept of Fourier integrals as follows.

¹See Priestley (1981a, p. 188-189) for the regularity conditions. The assumed period length 2π comes without loss of generality as the result is easily extended to period lengths other than 2π by a simple time scale transformation (Priestley, 1981a, p. 194).

²As Priestley (1981a, p. 187-188) points out, a direct proof of existence of (2.1) is extremely difficult. The usual way to come up with this expression is to *define* sequences $\{a_n\}$ and $\{b_n\}$ as given in equations (2.2) - (2.3). Then it can be shown that, under the assumptions given in Result 2.2.1, the right-hand side does indeed converge to $X(t)$.

Result 2.2.2 Fourier integrals

Priestley (1981a, p. 199-201)

Let $X(t)$ be a real valued, deterministic, and absolutely integrable non-periodic function fulfilling same regularity conditions as in Result 2.2.1. Then $\forall t$ $X(t)$ can be expressed as an integral of complex exponential:

$$X(t) = \int_{-\infty}^{\infty} p(f)e^{2\pi i f t} df \quad (2.4)$$

where

$$p(f) = \int_{-\infty}^{\infty} X(t)e^{-2\pi i f t} dt \quad (2.5)$$

Equation (2.5) is usually referred to as the *Fourier transform* of $X(t)$, and (2.4) is called the Fourier integral representation of function $X(t)$ or simply *inverse Fourier transform*. Together the two equations are known as a *Fourier pair*. It is worth noting that the only real difference between Fourier series and Fourier integral is that whereas a periodic function can be expressed as a sum of sinusoids over a discrete set of frequencies, a non-periodic function can only be expressed over a continuous frequency interval (Priestley, 1981a, p. 6).³ Result 2.2.2 could be generalized to treat also complex-valued function $X(t)$. However, as our analysis will focus solely on economic time series, the real-valued case is enough for our needs.

So far we have treated functions $X(t)$ and $p(f)$ as purely mathematical objects. There is, however, a very straightforward and natural way to attach physical meaning to the Fourier pair. $X(t)$ can be understood as (at this point still deterministic) process evolving over time, so that t represent an arbitrary point in time. On the other hand, f can be thought to represent *frequency*, that is, cycles per unit time. Then the two equations in Fourier pair (2.4) - (2.5) constitute a *mapping between time and frequency domains*.

Often in literature "ordinary" frequency f is replaced by "angular" frequency ω , indicating angular displacement per unit time. In this case the Fourier pair can be defined to have the form (Priestley, 1981a, p. 201)

³There actually exists a common Fourier representation for both periodic or non-periodic functions $X(t)$ using the so-called Fourier-Stieltjes integral

$$X(t) = \int_{-\infty}^{\infty} e^{i2\pi f t} dP(\omega) \quad ,$$

where $P(\omega)$ is a possibly complex valued function, called the Fourier-Stieltjes transform of $X(t)$, whose form can be determined from $X(t)$ (Priestley, 1981a, p. 6). As the approach of this thesis is more empirical than theoretical, we will not concern ourselves with this more general representation.

$$X(t) = \frac{1}{\sqrt{2\pi}} \int_{-\infty}^{\infty} G(f)e^{i\omega t} d\omega \quad (2.6)$$

$$G(\omega) = \frac{1}{\sqrt{2\pi}} \int_{-\infty}^{\infty} X(t)e^{-i\omega t} dt \quad (2.7)$$

Comparing (2.6) - (2.7) to (2.4) - (2.5), we notice that changing from ordinary frequency f to angular frequency ω introduces a scaling term $\frac{1}{\sqrt{2\pi}}$ in both Fourier pair equations. However, this a matter of convention; it would also be valid to define the Fourier pair as (WolframMathWorld, 2017)

$$X(t) = \int_{-\infty}^{\infty} G(f)e^{i\omega t} d\omega$$

$$G(\omega) = \frac{1}{2\pi} \int_{-\infty}^{\infty} X(t)e^{-i\omega t} dt$$

or

$$X(t) = \frac{1}{2\pi} \int_{-\infty}^{\infty} G(f)e^{i\omega t} d\omega$$

$$G(\omega) = \int_{-\infty}^{\infty} X(t)e^{-i\omega t} dt$$

In these cases, however, the symmetry between the Fourier transform and its inverse is broken, due to which definition (2.6)-(2.7) is sometimes preferred.

At this point we are still uninformed what $G(\omega)$ actually portrays, and further, what is achieved with the mapping between time and frequency domains. To answer these questions, we define two important concepts: energy and power of $X(t)$.

Definition 2.2.1 Energy and power

Priestley (1981a, p. 195, 204)

Let $X(t)$ be a deterministic (either periodic or non-periodic) function. Then its energy over the interval $[-T, T]$, denoted as $\mathcal{E}_{(-T, T)}$, is defined as

$$\mathcal{E}_{(-T, T)} = \int_{-T}^T X^2(t) dt \quad (2.8)$$

In turn, power, denoted by $\mathcal{P}_{(-T, T)}$, is defined as energy over unit time:

$$\mathcal{P}_{(-T, T)} = \frac{\mathcal{E}_{(-T, T)}}{2T} \quad (2.9)$$

Energy is a very common concept e.g. in electrical engineering, where we could want to capture the amount of energy dissipated when current runs through a circuit with unit resistance. For our application it is less clear what kind of meaning energy and power of $X(t)$ have. We will, however, shortly see what use they are to us.

As the last Result for this subsection we present the so-called Parseval's relation:

Result 2.2.3 Parseval's relation for periodic and non-periodic functions

Priestley (1981a, p. 195, 201)

Consider function $X(t)$ and coefficients a_n and b_n from Result 2.2.1. Then it holds that

$$\int_{-\infty}^{\infty} X^2(t)dt = \pi \left[\frac{1}{2}a_0^2 + \sum_{n=1}^{\infty} (a_n^2 + b_n^2) \right]$$

Next, consider functions $X(t)$ and $G(\omega)$ from equations (2.6) and (2.7). Then it holds that

$$\int_{-\infty}^{\infty} X^2(t)dt = \int_{-\infty}^{\infty} |G(\omega)|^2 d\omega$$

Parseval's relation tells us that Fourier transform is an energy-preserving transformation.⁴ That is, we can equivalently talk about energy spread out over a time interval or over a frequency interval. As Priestley (1981a, p. 204) puts it, " $\{|G(\omega)|^2 d\omega\}$ represents the contribution to the total energy from those components of $X(t)$ whose frequencies lie between ω and $\omega + d\omega$." Thus, quantity $|G(\omega)|^2$ measures the density of energy in a similar fashion as probability density function measures the density of a particular probability measure.

The last part of the puzzle is that "energy carried by a sine or cosine term is proportional to the square of the amplitude" (Priestley, 1981a, p. 9). That is, the greater the amplitude of a sinusoid, the greater the energy of that sinusoid, and vice versa. This is to say that if a sinusoid operating at frequency ω_0 has a large amplitude (or equivalently, large energy) compared to other driving sinusoids operating at different frequencies, then we can deduce that the most important source of swings in $X(t)$ is due to oscillations taking place at frequency ω_0 . We can reformulate this observation more compactly as the most important theoretical insight for our analysis:

By decomposing $X(t)$ into its frequency-domain components via Fourier transform, we can search for frequencies that influence changes in $X(t)$ the most.

⁴Depending on the scaling of the Fourier integrals, Parseval's relation might take slightly differing forms.

2.2.2 Family portrait of discrete-time Fourier transforms

So far we have established the connection between time and frequency domains for an aperiodic, continuous function $X(t)$ defined over the range $t \in (-\infty, \infty)$. This connection was the Fourier pair (2.6) and (2.7). However, in real life time series analysis we never come across such creatures, as we can measure a given variable only in finite chunks *and* at chosen sampling rate. Thus, the Fourier transform (2.7) is unsuitable for empirical analysis. To treat these challenges, we first introduce the so-called *Discrete Time Fourier Transform* (DTFT), which is essentially a version of the Fourier transform for discretely sampled time series. Imagine we now have an aperiodic, discrete function with uniformly spaced observations ($t = \dots - 2, -1, 0, 1, 2, \dots$) in our disposal. This effectively means that we are dealing with a *time series* instead of a continuous function having time as its argument. We will distinguish a time series from a continuous function by writing $\{X\}_t$. Now we can define the DTFT as follows.

Definition 2.2.2 *Discrete Time Fourier Transform and its inverse*
(Oppenheim, 2017)

The Discrete Time Fourier Transform (DTFT) of time series $\{X\}_{t=-\infty}^{\infty}$, v_X , is defined on interval $-\pi \leq \omega \leq \pi$ as

$$v_X(\omega) = \frac{1}{\sqrt{2\pi}} \sum_{t=-\infty}^{\infty} X_t e^{-i\omega t} \quad (2.10)$$

Further, the inverse DTFT is given by

$$X_t = \frac{1}{\sqrt{2\pi}} \int_{-\pi}^{\pi} v_X(\omega) e^{-i\omega t} d\omega$$

The analogy to Fourier integrals is clear; in (2.10) we have replaced the continuous time integral of (2.7) with a sum over discrete time periods. An interesting property of the DTFT is that it is periodic of length 2π . Further, in Definition 2.2.2 the scaling term has again been distributed evenly across the two equations, but as with Fourier integrals, it would be valid to scale the DTFT by $\frac{1}{2\pi}$ and its inverse by 1, or vice versa.

Although a step to right direction, DTFT still leaves us unsatisfied as it deals with series of infinite length. In practice, we will only have some sample of length N from the time series in our disposal. We will call such sample a *signal*. This effectively corresponds to a situation where we, instead of a time series of infinite length, consider a truncated version of $\{X\}_t$, namely

$$X_{M,t} = \begin{cases} X_t & \text{if } -M \leq t \leq M \\ 0 & \text{otherwise} \end{cases}$$

where $N = 2M + 1$. Replacing X_t in (2.10) by $X_{M,t}$ yields

$$\begin{aligned} \nu_{X_M}(\omega) &= \frac{1}{\sqrt{2\pi}} \sum_{t=-\infty}^{\infty} X_{M,t} e^{-i\omega t} \\ &= \frac{1}{\sqrt{2\pi}} \sum_{t=-M}^M X_{M,t} e^{-i\omega t} \end{aligned} \quad (2.11)$$

Equation (2.11) is essentially a "truncated" or "finite" Fourier transform in the sense that it is a finite-sample equivalent of (2.10). However, usually in literature a creature called *Finite Fourier Transform* (FFT) is defined with different indexing convention. In this text we define FFT as follows:⁵

Definition 2.2.3 *Finite Fourier Transform*

(Priestley, 1981a, p. 418)

Consider a signal with observations X_1, \dots, X_N at uniform intervals. We define the *Finite Fourier Transform*, ξ_X , as

$$\xi_X(\omega) = \frac{1}{\sqrt{2\pi}} \sum_{t=1}^N X_t e^{-i\omega t} \quad , -\pi \leq \omega \leq \pi \quad (2.12)$$

Although (2.11) and (2.12) seemingly differ, we can show that they are equivalent up to a (complex-valued) constant. To see this, we will use the *shift property of FFT*. Consider that we take the $2M + 1$ observations from (2.11) and assign them into a vector X of length $2M + 1$, where indexing runs from 1 to $2M + 1$.⁶ Let us denote a *circular shift of X by m steps to the right* as $X^{[-m]}$ (see section A.1 in Appendix about circular shifting). Then for every value in the circularly shifted vector $X^{[-m]}$ (at position n) we have that

$$X_n^{[-m]} \equiv X_{\langle n-m \rangle_N} \quad \forall n \quad ,$$

where notation $\langle k \rangle_N$ denotes the remainder of division k/N (see again section A.1), and X_i on the right-hand side is to be understood as a value at position i in vector X . Using the circularly shifted values, we are ready to introduce the shift property.

⁵Unlike Priestley (1981a) we don't scale the FFT with $\frac{1}{\sqrt{N}}$.

⁶That is, vector value at position $n = 1$ corresponds to X_{-M} of equation (2.11), $n = 2$ corresponds to $X_{-(M+1)}$, and so forth. The final value in vector X at position $n = 2M + 1$ corresponds to X_{M+1} .

Result 2.2.4 Shift property of FFT

(dsprelated.com, 2017)

For FFT in (2.12) it holds that

$$\xi_{X^{[-m]}}(\omega) = e^{-i\omega(-m)}\xi_X(\omega) \quad (2.13)$$

That is, FFT of circularly shifted signal coincides with the FFT of the original signal multiplied by linear phase $e^{-i\omega m}$.

Now let us perform a change of variable $t = t' - (M + 1)$ such that equation (2.11) can be rewritten as⁷

$$\begin{aligned} v_{X_M}(\omega) &= \frac{1}{\sqrt{2\pi}} \sum_{t=-M}^M X_{M,t} e^{-i\omega t} \\ &= \frac{1}{\sqrt{2\pi}} \sum_{t'=1}^N X_{M,t'-(M+1)} e^{-i\omega(t'-(M+1))} \\ &= e^{i\omega(M+1)} \frac{1}{\sqrt{2\pi}} \sum_{t'=1}^N X_{M,t'-(M+1)} e^{-i\omega t'} \\ &= e^{i\omega(M+1)} \frac{1}{\sqrt{2\pi}} \sum_{t'=1}^N X'_{M,t'} e^{-i\omega t'} \quad | \text{ eq. (2.12)} \\ &= e^{-i\omega(-(M+1))} \xi_{X'_{M,t}} \end{aligned}$$

where $N = 2M + 1$ and $X'_{M,t}$ is a linearly shifted version of vector $X_{M,t}$.⁸ Thus, the truncated DTFT in (2.11) is just FFT in (2.12) scaled with linear phase, and from (2.13) we further deduce that

$$v_{X_M}(\omega) = \xi_{X_M^{[-(M+1)]}}(\omega) \quad (2.14)$$

This means that in order to calculate the truncated DTFT in (2.11), we can simply *calculate the FFT of circularly shifted ($M + 1$ steps to right) version of vector X_M* . Due to their similarity, from here on we will refer to the truncated DTFT as Finite Fourier Transform (FFT).

⁷I am thankful for user *msm* in Signal Processing forum of Stack Exchange for proposing this derivation (stackexchange.com, 2017).

⁸Linear shift means simply that we shift indexing. Values in the linearly shifted vector are in the same order as in the original vector.

Although we now have a tool to handle a discrete and finite sample from a time series, we still face a problem regarding the practical implementation as FFT is defined over a continuous frequency range $-\pi \leq \omega \leq \pi$. This is something that computers struggle to cope with, as the world they live in is inherently discrete. Thus, we need yet another version of the Fourier transform that is defined over a discrete set of frequencies. This version goes by the name *Discrete Fourier Transform* (DFT):

Definition 2.2.4 *Discrete Fourier Transform and its inverse*

(Mathworks, 2017)

Consider a signal $X_t, t = 1, \dots, N$. Let also $k = 1, \dots, N$. Then we can define the Discrete Fourier Transform of $X_t, \eta_{X,k}$, as

$$\eta_{X,k} = \sum_{t=1}^N X_t e^{-i \frac{2\pi(k-1)}{N}(t-1)} \quad (2.15)$$

with the inverse DFT taking the form

$$X_t = \frac{1}{N} \sum_{k=1}^N \eta_{X,k} e^{i \frac{2\pi(k-1)}{N}(t-1)}$$

DFT is a very useful equation and is baked into virtually all statistical software. It allows a straightforward way to calculate a discrete-valued estimation for continuously valued FFTs. There are certain things that are worth noting. First, we let the indices t and k run from 1 to N (instead of 0 to $N - 1$ as it often is the case) to make the numerical implementation in Matlab easier. Second, continuous argument ω of FFT has been replaced with discrete points $\omega_k \equiv \frac{2\pi(k-1)}{N}$. Third, DFT is periodic with length N . Lastly, unlike with Fourier integrals and DTFT above, the DFT and its inverse are defined such that there is a scaling term appearing only in the inverse.⁹ This choice is made to match the convention used in Matlab in the implementation of the DFT (Mathworks, 2017).

Practically speaking, whenever we want to evaluate some FFT, we use the DFT as in (2.15) and scale the output to match the chosen definition for the FFT. For example, if we were to calculate FFT as defined in (2.12), we would employ the DFT as in (2.15) and scale the resulting output by $\frac{1}{\sqrt{N}}$.

⁹Here scaling term $\frac{1}{N}$ corresponds to the term $\frac{1}{2\pi}$ of continuously valued DTFT and FFT.

2.3 Spectral analysis of stationary processes

2.3.1 Univariate spectrum

In section 2.2 we dealt only with deterministic processes. This, of course, is not totally satisfactory as the world Economists live in is inherently random. The goal of this section is to extend the ideas developed so far to treat stochastic settings. Throughout the section we will be working with a weakly stationary stochastic process $\{X(\omega)\}_t$, where $\omega \in \Omega$ represents a probability singleton, and Ω constitutes the probability space (Ω, \mathcal{F}, P) . As the naming conventions of probability theory and spectral analysis unfortunately coincide (ω indicating both angular frequency and probability singleton), we denote a probability singleton as α . Thus, following the usual convention, we write $X(t, \alpha)$ either for a single \mathcal{F} -measurable random variable or for the stochastic process (i.e. collection of random variables) whenever the meaning is obvious from the context.¹⁰ $X(t)$ will refer to some realization of random variable $X(t, \alpha)$

Similar to the deterministic case, we want to construct a Fourier representation for a stationary stochastic process $X(t, \alpha)$. However, there are problems that immediately face us:

1. How do we deal with the fact that a stochastic process can have multiple realizations?
2. Stationary process $X(t, \alpha)$ does not die away, i.e. is not absolutely integrable.

Focusing on the first point, we will for now consider some certain realization path of the stochastic process $X(t, \alpha)$, namely $X(t, \alpha^*)$. To treat the second problem, Priestley (1981a, p. 207) considers a truncated version of $X(t, \alpha^*)$ of the form

$$X_T(t, \alpha^*) = \begin{cases} X(t, \alpha^*) & , \text{ if } -T \leq t \leq T \\ 0 & , \text{ otherwise} \end{cases}$$

where the crucial condition of absolute integrability is (trivially) fulfilled. In this case we can construct a representation akin to (2.6)-(2.7) for $X_T(t, \alpha^*)$, namely

$$X_T(t, \alpha^*) = \frac{1}{\sqrt{2\pi}} \int_{-\infty}^{\infty} G(f) e^{i\omega t} d\omega \quad (2.16)$$

¹⁰When we want to differentiate between a single random variable and a stochastic process we write $X(t, \alpha)$ for the random variable and $\{X(\alpha)\}_t$ for the stochastic process.

and

$$\begin{aligned} G(\omega) &= \frac{1}{\sqrt{2\pi}} \int_{-\infty}^{\infty} X_T(t, \alpha^*) e^{-i\omega t} dt \\ &= \frac{1}{\sqrt{2\pi}} \int_{-T}^T X_T(t, \alpha^*) e^{-i\omega t} dt \end{aligned} \quad (2.17)$$

Here $|G_T(\omega)|^2$ has the same interpretation as in section 2.2.1, i.e. the energy density function of $X_T(t, \alpha^*)$. This interpretation, however, gives rise to a third major problem:

3. $\lim_{T \rightarrow \infty} |G_T(\omega)|^2$ is not finite (i.e. does not exist), and hence we cannot meaningfully talk about energy distribution over the whole interval $(-\infty, \infty)$.

To treat this problem, Priestley (1981a, p. 208) instructs to look at power instead of energy, which suggests to consider expression

$$\lim_{T \rightarrow \infty} \frac{|G_T(\omega)|^2}{2T}$$

To allow the possibility of multiple realizations (and hence treat the first problem), we introduce the expectation operator into the above equation, giving the following definition.

Definition 2.3.1 Power Spectral Density

Priestley (1981a, p. 208)

The power spectral density function $h(\omega)$ of stationary stochastic process $X(t, \alpha)$ is defined as

$$h(\omega) \equiv \lim_{T \rightarrow \infty} E \left[\frac{|G_T(\omega)|^2}{2T} \right] \quad (2.18)$$

When $h(\omega)$ exists, $h(\omega)d\omega$ has the interpretation of being the "average (over all realizations) of the contribution to the total power from components in $X(t)$ with frequencies between ω and $\omega + d\omega$ " (Priestley, 1981a, p 208).¹¹ For this reason $h(\omega)$ is usually referred to as the power density function of $X(t, \alpha)$.¹²

¹¹For this interpretation to be completely valid, we actually need a more general type of Fourier expansion that is able to represent the complete realization interval ($t = -\infty$ to ∞) instead of the Fourier integral over finite interval ($t = -T$ to T) in (2.16). Luckily such representation does indeed exist. This result is due to the so-called *Spectral Representation Theorem*. For a thorough discussion, see Priestley (1981a, p. 244).

¹²To be completely accurate, what is referred to as the power density function is the normalized version $\frac{h(\omega)}{\sigma_X^2}$, as it has the same properties as probability density function. However, for our analysis the normalization is not relevant.

Although summarizing what spectral density is about, Definition 2.3.1 does not provide a straightforward tool for calculating $h(\omega)$. Fortunately, given (2.18), the Fourier transform lends itself yet again to our use by permitting a representation that bridges the time-domain and frequency-domain analyses by linking the autocovariance function $\gamma(r)$ of $X(t, \alpha)$ to the spectral density $h(\omega)$ as follows:

Result 2.3.1 Relationship between spectral density and autocovariances

Priestley (1981a, p. 210-225)

In continuous time case, the autocovariance sequence $\gamma(\tau)$ ($\tau \in (-\infty, \infty)$) of $X(t, \alpha)$ is linked to the spectral density function $h(\omega)$ of $X(t, \alpha)$ via Fourier pair representation

$$h(\omega) = \frac{1}{2\pi} \int_{\tau=-\infty}^{\infty} \gamma(\tau) e^{-i\omega\tau} d\tau \quad (2.19)$$

$$\gamma(\tau) = \int_{-\infty}^{\infty} h(\omega) e^{i\omega\tau} d\omega \quad (2.20)$$

In discrete time case, the autocovariance sequence $\gamma(r)$ ($r = 0, \pm 1, \pm 2, \dots$) of $X(t, \alpha)$ is linked to the spectral density function $h(\omega)$ of $X(t, \alpha)$ via discrete-time Fourier pair representation

$$h(\omega) = \frac{1}{2\pi} \sum_{r=-\infty}^{\infty} \gamma(r) e^{-i\omega r} \quad -\pi \leq \omega \leq \pi \quad (2.21)$$

$$\gamma(r) = \int_{-\pi}^{\pi} h(\omega) e^{i\omega r} d\omega \quad , r = 0, \pm 1, \pm 2 \dots \quad (2.22)$$

These results are special cases of the so-called Wiener-Khintchine Theorem and Wold's Theorem, see Priestley (1981a, p. 219, 222). What they state is that we can obtain the spectral density of (either continuously or discretely valued) $X(t, \alpha)$ by applying the Fourier transform to the autocovariance function of $X(t, \alpha)$.

2.3.2 Cross-spectrum

Above we saw that autocovariances and spectral density are essentially two sides of the same coin. The generalization to multivariate case is rather straightforward. As we are able to investigate co-movement of two series in time-domain using their cross-covariances, we would expect there to be a natural extension to the spectral density as well, a sort of *cross-spectral density* that would summarize the co-movement of the two series in

frequency-domain. This indeed is the case, and the multivariate version corresponding to (2.21) - (2.22) are given by (Priestley, 1981b, p. 667)

$$h_{ij}(\omega) = \frac{1}{2\pi} \sum_{r=-\infty}^{\infty} \gamma_{ij}(r) e^{-i\omega r} \quad -\pi \leq \omega \leq \pi \quad (2.23)$$

$$\gamma_{ij}(r) = \int_{-\pi}^{\pi} h_{ij}(\omega) e^{i\omega r} d\omega \quad , r = 0, \pm 1, \pm 2 \dots \quad (2.24)$$

where i refers to stochastic process $X_i(t, \alpha)$ and j to $X_j(t, \alpha)$, $\gamma_{ij}(r)$ is the cross-covariance function, and $h_{ij}(r)$ is referred to as the cross-spectral density.

2.4 Estimation of spectral densities

In previous section we laid out the theoretical concepts for spectral analysis. Now the task is to see how these concepts are employed in a real-world setting. That is, we want a practical cook-book recipe how to obtain estimates for spectral densities using only a finite amount of observations. In this section we first develop two "natural" estimators for the spectral density and see why they are not getting the job done. We then improve our estimators by introducing a method called windowing.

2.4.1 Univariate natural estimators

Our goal in this subsection is to obtain an estimate for the spectral density $h(\omega)$.¹³ It turns out there are many ways to achieve this. To begin our estimation process, we must first choose between parametric and non-parametric methods. Like the name suggests, parametric methods involve choosing a pre-fixed model with certain parameters, which then is fitted to data. Using the properties of the fitted model one can estimate statistical features of interest. On the contrary, non-parametric methods are "parameter free" in the sense that no *a priori* assumptions about the functional form of the model are made. In this thesis we will consider perhaps the two most common non-parametric spectral estimators, called *periodogram* and *correlogram* (Stoica and Moses, 2004, p. 22). These estimators can be thought of as "natural" estimators of $h(\omega)$ as they are directly linked to the population-based equations (2.18) and (2.21).

We start by defining the periodogram. For the sake of the conversation below, we consider to have a finite sample of N observations X_0, X_1, \dots, X_{N-1} , drawn from time series $\{X\}_t$, in our disposal.

¹³We will assume that $h(\omega)$ is continuous for all ω . This will be fulfilled if $\gamma(r)$ is absolutely summable (Priestley, 1981a, p. 416). Most of the common processes (AR, ARMA) have continuous spectra.

Definition 2.4.1 Periodogram

Priestley (1981a, p. 395)

Given N observations X_0, X_2, \dots, X_{N-1} drawn from stochastic process $X(t, \alpha)$, function $I_N(\omega)$, called the periodogram, is defined for all ω in the range $-\pi \leq \omega \leq \pi$ as

$$I_N(\omega) = \frac{2}{N} \left| \sum_{t=1}^N X_t e^{-i\omega t} \right|^2$$

Recall now Definition 2.3.1 for the power spectral density, which is essentially the expected value of squared Fourier transform of continuous time parameter function $X(t, \alpha)$, taken to the limit. The periodogram is the same thing but adapted to finite case. To see this, consider that since we now have only N discrete observations instead of a continuous range of observations, we can in equation (2.18) replace the term $2T$ (representing the length of the interval) with N . Furthermore, we can neglect the expectation and limit operators since the only available information on $X(t, \alpha)$ is the finite sample X_1, \dots, X_N (Stoica and Moses, 2004, p. 22). To conclude that the periodogram is just a (scaled) squared value of the FFT in (2.12), notice that

$$\begin{aligned} I_N(\omega) &= \frac{2}{N} \left| \sum_{t=1}^N X_t e^{-i\omega t} \right|^2 \\ &= \frac{4\pi}{2\pi N} \left| \sum_{t=1}^N X_t e^{-i\omega t} \right|^2 \\ &= \frac{4\pi}{N} \left| \frac{1}{\sqrt{2\pi}} \sum_{t=1}^N X_t e^{-i\omega t} \right|^2 \\ &= \frac{4\pi}{N} |\xi_X(\omega)|^2 \end{aligned} \tag{2.25}$$

If we define the "modified periodogram" (Priestley, 1981a, p. 416) as $I_N^* \equiv \frac{N}{4\pi} I_N(\omega)$, then we can write our first "natural" estimator, $\hat{h}^P(\omega)$, of spectral density $h(\omega)$ as

$$\hat{h}^P(\omega) \equiv I_N^*(\omega) = |\xi_X(\omega)|^2 \tag{2.26}$$

Now we turn to the second "natural" estimator, i.e. the correlogram. Recall equation (2.21) which is a population-based equation linking the spectral density to autocovariances. If we in (2.21) replace the population autocovariance function $\gamma(r)$ with its (biased) sample estimator

$$\hat{\gamma}(r) = \frac{1}{N} \sum_{t=1}^{N-|r|} (X_t - \mu)(X_{t+|r|} - \mu) \quad ,$$

where μ denotes the sample average of X_t , we obtain the correlogram estimator $\hat{h}^c(\omega)$ of spectral density $h(\omega)$:¹⁴

$$\begin{aligned} \hat{h}^c(\omega) &= \frac{1}{2\pi} \sum_{r=-\infty}^{\infty} \hat{\gamma}(r) e^{-i\omega r} \\ &= \frac{1}{2\pi} \sum_{r=-(N-1)}^{N-1} \hat{\gamma}(r) e^{-i\omega r} \end{aligned} \quad (2.27)$$

That is, $\hat{h}^c(\omega)$ is the (scaled) FFT of the autocovariance estimates.

At this point we have developed our two "natural" estimators $\hat{h}^p(\omega)$ and $\hat{h}^c(\omega)$. As they both estimate the same quantity, it is not totally surprising that they can be shown to coincide with each other¹⁵, i.e.

$$\hat{h}^p(\omega) = \hat{h}^c(\omega)$$

Although the estimators are mathematically equivalent, they offer different viewpoints in a similar way population based equations (2.18) and (2.21) do. However, we are still not done. In fact, our natural estimators are actually poor estimators of the actual (continuous) spectral density $h(\omega)$! Priestley (1981a, p. 429 - 432) and Stoica and Moses (2004, p. 25) discuss in length why this is the case. A short answer is that, looking from the perspective of $\hat{h}^c(\omega)$ in (2.27), with values of $|r|$ close to $N - 1$ the autocovariances are poorly estimated. Sometimes it is said that the tail autocovariances exhibit too "wild" a behaviour (Priestley, 1981a, p. 432), consequence of which is that the spectral density estimator exhibits too large a variance to be considered as providing good enough estimates for $h(\omega)$. To remedy this we would have to come up with a way to reduce the effect of the "tail" autocovariances in our estimation process. This procedure will be discussed in the next sub-section.

2.4.2 Consistent estimation of univariate spectrum

To overcome the problem of natural estimators being too erratic, many different methods have been proposed in the literature. Stoica and Moses (2004, ch. 2.5 - 2.7) offer a

¹⁴Stoica and Moses (2004, p. 23) discuss why biased sample estimates are usually used in conjunction with spectral analysis instead of unbiased estimates.

¹⁵See Priestley (1981a, p. 416, 435) or Stoica and Moses (2004, p. 24)

summary of these methods. One of the most earliest approaches is the so-called *Bartlett method* (Bartlett, 1948). The idea in Bartlett method is to split the data into sub-samples of equal length, and average the periodograms calculated over each sub-sample. A refined version of the same idea is due to Welch (1967), with the additions being that sub-samples are allowed to overlap, and a certain window function is applied to the sub-sample values before the periodogram is computed. Welch's method is widely used; *inter alia*, it is the default approach adopted in Matlab's Signal Processing toolbox.

However, in this thesis we will highlight the so-called *Blackman-Tukey method* (Blackman and Tukey, 1958) which will be used in our empirical work. The main reason for choosing this particular estimation method is to obtain as comparable results as possible with Schüler et al. (2015). Furthermore, the Blackman-Tukey approach is fairly intuitive, as it explicitly treats the problem of "wild" tail autocovariances by introducing a lag window truncating the tails of the autocovariance function from the estimation procedure. Formally, in the Blackman-Tukey method we consider a modified version of the estimator in (2.27):

Definition 2.4.2 *Blackman-Tukey estimator*

Stoica and Moses (2004, p. 37), Priestley (1981a, p. 434)

Given sample estimates $\hat{\gamma}(r)$ for autocovariance function $\gamma(r)$ of $X(t, \alpha)$, the Blackman-Tukey estimator of spectral density $h(\omega)$ is defined as

$$\hat{h}(\omega)^{BT} = \frac{1}{2\pi} \sum_{r=-(N-1)}^{N-1} \lambda(r) \hat{\gamma}(r) e^{-i\omega r} \quad (2.28)$$

where $\lambda(r)$ is some even function¹⁶ that decays smoothly to zero with r , i.e. there exists $M < N - 1$ such that, for $|r| > M$, $\lambda(r) = 0$.

We can see that $\lambda(r)$ acts as a weighting function, applying decreasing weights to autocovariances with greater lags, and for $|r| > M$ effectively truncating the corresponding autocovariances. For this reason $\lambda(r)$ is usually referred to as the *lag window*.

It is instructive to write (2.28) in a slightly differing form. Let us denote the (scaled) FFT of $\lambda(r)$ as $W(\omega)$, i.e.

$$W(\omega) = \frac{1}{2\pi} \sum_{s=-(N-1)}^{N-1} \lambda(s) e^{-i\omega s}$$

¹⁶That is, $\lambda(-s) = \lambda(s)$ such that $\lambda(0) = 1$.

Then it is straightforward to show that (Priestley, 1981a, p. 435)

$$\hat{h}(\omega)^{BT} = \int_{-\pi}^{\pi} \bar{h}^p(\theta) W(\omega - \theta) d\theta$$

This means that we can write the Blackman-Tukey estimator as a locally weighted average of the periodogram estimator. The intuition is that we can reduce the erratic behaviour of the periodogram by locally averaging it over a continuous range of frequencies. This is equivalent to reducing the significance of tail covariances by applying a lag window in time-domain. Since $W(\theta)$ operates in the same manner for the periodogram as $\lambda(r)$ for the autocovariances, $W(\theta)$ is often referred to as a "spectral window"; it offers a view on the periodogram through a narrow window from $\omega - \epsilon$ to $\omega + \epsilon$ (Priestley, 1981a, p. 436). $W(\theta)$ assigns effectively zero weights to $\hat{h}^p(\theta)$ when θ escapes some interval $(-\epsilon, \epsilon)$ centered at ω , i.e. when the distance $|\omega - \theta|$ becomes greater than the fixed distance $|\omega - \epsilon|$ (Priestley, 1981a, p. 436).

Given our discussion above, it is clear that the choice of $\lambda(r)$, or equivalently $W(\omega)$, is crucial for the performance of \hat{h}^{BT} as an estimator. So far we haven't said anything concrete about the actual form of either one. As $\lambda(r)$ and $W(\omega)$ constitute a Fourier pair, it is obvious that if we specify the functional form of either one we will also define the functional form of the other. There are many different possibilities how to select these window functions, and no attempt is made here to give an exhaustive list. Instead, we introduce one particular choice which will be used in our empirical analysis in Chapter 3. For an extensive exposition for different choices of lag and spectral windows one can turn to section 6.2.3 of Priestley (1981a).

The lag window introduced here is the so-called *Parzen lag window*, defined as (Priestley, 1981a, p. 443)

$$\lambda(r) = \begin{cases} 1 - 6\left(\frac{r}{M}\right)^2 + 6\left(\frac{|r|}{M}\right)^3 & \text{for } |r| < \frac{M}{2} \\ 2\left(1 - \left|\frac{r}{M}\right|^3\right) & \text{for } \frac{M}{2} \leq r \leq M \\ 0 & \text{otherwise} \end{cases}$$

An important decision is how to select the truncation parameter $M < N - 1$ as it brings about a trade-off between resolution and statistical variance of the spectral density estimator (Stoica and Moses, 2004, p. 41). Alternatively, there is a trade-off between variance and bias. Table 2.1 illustrates these trade-offs, and Figure 2.1 depicts Parzen lag window with truncation parameter $M = 69$. We will discuss the selection of M in more detail in section 3.3.

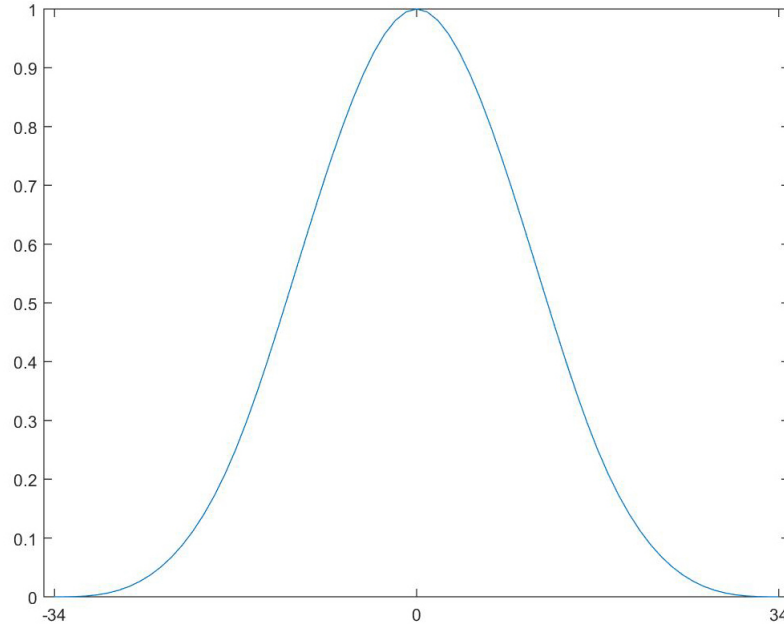


Figure 2.1: Parzen lag window with truncation parameter $M = 69$.

$M \uparrow$	variance \uparrow	bias \downarrow	resolution \downarrow
$M \downarrow$	variance \downarrow	bias \uparrow	resolution \uparrow

Table 2.1: How increasing/decreasing M affects properties of $\hat{h}(\omega)^{BT}$.

2.4.3 Multivariate estimators

We can straightforwardly generalize the univariate estimators to treat the multivariate case. Consider we have S stationary time series $\{X_j\}_t, j = 1, \dots, S$, and we draw N observations from each of them. If we define the *modified periodogram matrix* as (Priestley, 1981b, p. 694)

$$\mathbf{I}_N^* \equiv \{I_{N,jh}^*\} \quad j, h = 1, \dots, S$$

such that

$$I_{N,jh}^* = \frac{1}{N} \xi_{X_j}(\omega) \xi_{X_h}^T(\omega) \quad ,$$

where T denotes conjugation and transposition, and $\forall j \xi_{X_j}(\omega)$ is defined as in (2.12), then the periodogram estimator matrix $\hat{\mathbf{h}}^P$ is given by

$$\hat{\mathbf{h}}^P = \mathbf{I}_N^* \tag{2.29}$$

The diagonal of $\hat{\mathbf{h}}^{\mathbf{P}}$ comprises of univariate spectral densities and off-diagonal elements represent cross-spectral densities. Similarly, the *matrix of correlogram estimators* is given by (Priestley, 1981b, p. 667)

$$\hat{\mathbf{h}}^{\mathbf{c}} = \frac{1}{2\pi} \sum_{r=-(N-1)}^{N-1} \hat{\gamma}(r) e^{-i\omega r} \quad ,$$

where matrix $\hat{\gamma}(r)$ comprises of cross-covariance estimators $\hat{\gamma}_{jh}$, i.e.

$$\hat{\gamma}(r) = \{\hat{\gamma}_{jh}(r)\} \quad j, h = 1, 2, \dots, S$$

$$\hat{\gamma}_{jh}(r) = \frac{1}{N} \sum_{t=1}^{N-|r|} (X_{j,t} - \mu_j)(X_{h,t+|r|} - \mu_h)$$

where $r = 0, \pm 1, \dots, \pm(N-1)$. μ_j and μ_h denote the sample averages of X_j and X_h .

For consistent estimation of the cross-spectral densities, we introduce the *Blackman-Tukey estimator matrix* as (Priestley, 1981b, p. 694)

$$\hat{\mathbf{h}}^{\mathbf{BT}}(\omega) = \frac{1}{2\pi} \sum_{r=-(N-1)}^{N-1} \lambda(r) \hat{\gamma}(r) e^{-i\omega r} \quad , \quad (2.30)$$

where the element (j, h) of $\hat{\mathbf{h}}^{\mathbf{BT}}(\omega)$ is given by

$$\hat{h}_{ij}(\omega) = \frac{1}{2\pi} \sum_{r=-(N-1)}^{N-1} \lambda(r) \hat{\gamma}_{jh}(r) e^{-i\omega r} \quad (2.31)$$

We see that the only difference to the univariate case (2.28) is that we have replaced the autocovariance estimator $\hat{\gamma}_{jj}(r)$ with the cross-covariance estimator $\hat{\gamma}_{jh}(r)$.

Chapter 3

Constructing Composite Financial Cycle

In this chapter we describe the construction of the Composite Financial Cycle, or CFC for short. Our approach here follows closely research conducted at the European Central Bank (Schüler et al., 2015). The goal is to derive a financial cycle proxy having the following properties:

1. Parsimonious description of developments in the underlying macro-financial sector.
2. Good predictor of periods of high financial stress.

In Chapter 4 we will test how well our CFC fares in explaining overheating in the macro-financial sector, and also compare our results with those of Schüler et al. (2015).

The construction of the CFC comes in four different phases, each of which will be covered in a separate section. First in Phase 1 (section 3.1) we discuss the selection of relevant variables for our analysis. Phase 2 (section 3.2) examines the aggregation of the chosen variables into a composite stress index, which will have a similar structure as the Composite Indicator of Systemic Stress à la Holló et al. (2012). Phase 3 (section 3.3) dives into the frequency-domain analysis. We become acquainted with the so-called Power Cohesion measure (PCoh) championed by Schüler et al. (2015), which is essentially a weighted average of cross-spectral densities. PCoh offers a way to endogenously identify a frequency band of most important co-movement across variables of interest. Lastly in Phase 4 (section 3.4), the stress index is filtered using a band-pass filter calibrated with the frequency band identified in Phase 3. Figure 3.1 summarizes the four steps.

3.1 Selecting relevant variables

As explained above, one of the desired properties of our financial cycle proxy is to predict financial stress. Hence, we want to include variables whose swings have the most

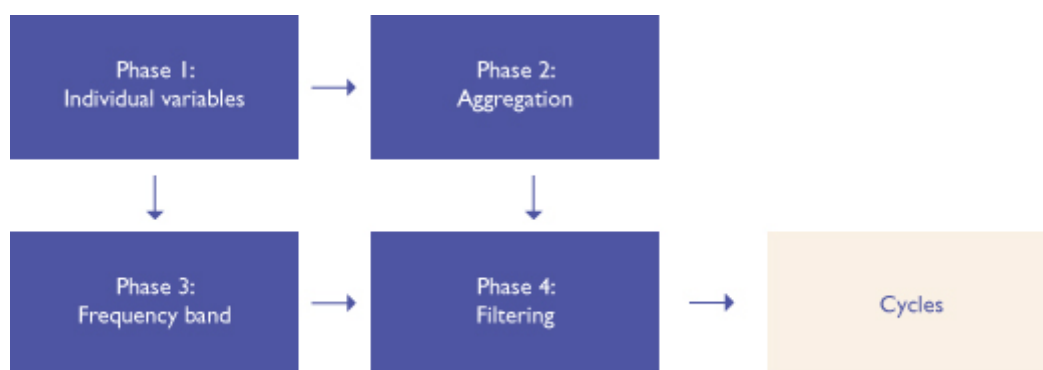


Figure 3.1: Roadmap to Chapter 3.

considerable effect to the macro-financial sector as a whole. We select our variables based on the frequency of appearance in the junction of strands of literature dealing with financial cycles and early warning indicators.¹

Similarly to Drehmann et al. (2012), we include private credit and house prices as our first two variables. Credit is a common guest in literature revolving around financial stability. Works such as Aikman et al. (2015), Schularick and Taylor (2012), and Geanakolpos (2010) have stressed the role of credit in determining swings in the financial conditions and asset prices. Importance of credit has not gone unnoticed in policy work either as it has been firmly baked into the Basel III regulation in the form of credit-to-GDP gap. On the other hand, the burst of the U.S. real-estate bubble in 2007-2008 exhibited how dire an effect negative developments in the residential sector can have on the economy. Third variable we include is local benchmark stock index. Swings in stock prices are associated with boom-bust cycles in the financial markets. Although Drehmann et al. (2012) find stock prices to be less-fitting when talking about financial cycles, later research (Schüler et al., 2015) has challenged this view by claiming that stock prices do share important common cyclicalities with credit and residential prices. Further, stock returns are often included in early warning exercises (Tölö et al., 2017). Further, Schüler et al. (2015, p. 3) also include the government benchmark 10-year bond yield in order to "complete... the portfolio set faced by economic agents". Thus, in order to derive comparable results, we also include bond yields.

Together these four variables are referred to as *financial cycle variables*. The raw series are fetched from sources such as BIS, ECB and OECD through Bank of Finland's database link. Table 3.1 provides a summary of the used variables and their mnemonics. For the rest of the text, variables are referred to with their mnemonics. A detailed list of series definitions and data sources is provided in section A.2 of Appendix.

¹For an excellent survey of most common variables in early warning exercises, please see Table 1 in Tölö et al. (2017).

Name	Mnemonic	Unit
Credit to non-fin. private sector	Credit	QoQ % changes
Residential property prices	House prices	QoQ % changes
Stock prices	Stocks	QoQ % changes
10y gov. bond yield	Bond yield	QoQ %-point changes

Table 3.1: Financial cycle variables used in constructing Composite Financial Cycles.

In order to use the variables in our analysis certain transformations are conducted. First, series that are originally expressed in nominal terms (credit and stocks) are deflated using country specific consumer price index. Section A.3 in Appendix presents the formal treatment of deflation. Secondly, variables need to be de-trended as spectral analysis can only deal with stationary series. De-trending is performed by simple differencing methods. Section A.4 in Appendix presents the formal treatment of differencing. Ultimately, credit, house prices, and stocks are presented as percentage changes. Bond yields are presented as percentage point changes. Finally, series for each country are truncated according to the shortest one. For example, if a country has data from 1970Q1 until 2016Q2 for three financial cycle variables but for the 4th one only from 1980Q2 until 2016Q2, then all variables for that country are truncated to the time interval 1980Q2-2016Q2. Table 3.2 provides a summary of the common time samples for the treated data series for each country in sample. We will denote the treated series as

$$\begin{aligned}
 I_1 &: \text{Credit} \\
 I_2 &: \text{House prices} \\
 I_3 &: \text{Stock prices} \\
 I_4 &: \text{Bond yield}
 \end{aligned}
 \tag{3.1}$$

so that $\{I_i\}_t$ is to be understood as a time series of i th variable.

3.2 Stress index

Phase two deals with the aggregation of chosen variables into a composite stress index. The method followed here was originally introduced by Holló et al. (2012), and modified for current context by Schöler et al. (2015). Ideally, the stress index indicates the amount of stress in the macro-financial sector at a given point in time. For a thorough discussion about the optimal design of stress indices, reader is instructed to e.g. Holló et al. (2012) and Huotari (2015). In general, the construction of a stress index involves three steps:

Country	Financial cycle variables
	QoQ differencing
AUT	1986Q4-2016Q2
BEL	1985Q3-2016Q2
DEU	1970Q2-2016Q2
DNK	1983Q4-2016Q2
ESP	1985Q2-2016Q2
FIN	1971Q4-2016Q2
FRA	1970Q2-2016Q2
IRL	1971Q3-2016Q1
ITA	1970Q4-2016Q2
NLD	1970Q2-2016Q2
PRT	1988Q2-2016Q2
SWE	1970Q2-2016Q2
GBR	1970Q2-2016Q2
EA	1987Q2-2016Q2

Table 3.2: Common time samples of financial cycle variables after treatments.

1. Pre-multiplying variables such that increases in their value translate to improvement in the macro-financial sector.
2. Normalization of variables.
3. Aggregation of variables.

Below we will treat each of these steps in separate subsections.

3.2.1 Pre-multiplying variables

As is common in related literature, we want an increase in the value of a variable to indicate improvement in macro-financial conditions. This also means that increases in the resulting CFC indicate improving conditions. Common stylized facts imply that rising credit and asset prices translate to improving economic conditions. Therefore, three from our four variables – credit, house prices, and stocks – already have the "right" sign, but as bond yields are inversely related to their price, we pre-multiply the bond yield values by -1 .

3.2.2 Normalizing variables

Before the financial cycle variables are aggregated into a composite stress index, they are normalized into a common scale in order to ensure comparability. In our work we follow Holló et al. (2012) and normalize the variables using the so-called *empirical cumulative distribution function* transformation, or ECDF transformation for short. When the ECDF transformation is performed on an arbitrary time series $\{X\}_t$, we denote the resulting normalized series as $\{z\}_t$. Similarly to Holló et al. (2012), we refer to z_i (i.e. the ECDF transformed financial cycle variable I_i) as *stress factor* as it constitutes one of the building blocks of the resulting stress index.

Let us formalize the normalization process. Consider we are given an arbitrary time series $\{X\}_t$ from which a finite sample of consecutive n observations $X = (X_1, X_2, \dots, X_n)$ has been drawn. Now order the observations into ascending order. We call the resulting ordered vector of values as *ordered sample* and we denote it as

$$\bar{X} \equiv (X_{[1]}, X_{[2]}, \dots, X_{[n]})$$

$r = 1, 2, \dots, n$ is referred to as the *ranking number* assigned to a particular realization.² \bar{X} has the property that $X_{[1]} \leq X_{[2]} \leq \dots \leq X_{[n]}$. That is, the first observation in \bar{X} , $X_{[1]}$, is the smallest of all sample observations and has the ranking number $r = 1$, the second, $X_{[2]}$, is second largest and has the ranking number $r = 2$, and so forth.

Assume first that our sample includes only distinct values, i.e. *there are no repeated values in the ordered vector*. In this case the ECDF transformed series $\{z\}_t$ is computed from $\{X\}_t$ as follows. For every $j \in [1, n]$, define the ECDF as

$$F_n(X_j) = \begin{cases} \frac{r}{n} & \text{for } X_{[r]} \leq X_t < X_{[r+1]}, r = 1, 2, \dots, n-1 \\ 1 & \text{for } X_t \geq X_{[n]} \end{cases} \quad (3.2)$$

The ECDF $F_n(x^*)$ measures the "total number of observations from time series $\{X\}_t$ not exceeding a particular value $X^* = r^*$ divided by the total number of observations in the sample" (Holló et al., 2012, p. 15). The transformation thus projects series into a unit-free ordinal scale with range $(0, 1]$, essentially mimicking a probability measure under which all events have a positive probability. Thus, we can project each drawn observation $X_j, j = [1, 2, \dots, n]$, into a transformed value z_j according to the rule

$$z_j = F_n(X_j) \quad \forall j \quad (3.3)$$

²Ranking number is distinguished from a time subscript by square brackets.

On the other hand, if the sample X includes repeating values, then the ECDF given in equation (3.2) has to be slightly modified.³ Repeating values appear back-to-back in the ordered sample and hence also have back-to-back ranking numbers. This in turn, by equation (3.3), would mean that repeating values are projected into differing transformed values. However, we wish to assign all repeated observations the same transformed value. We will achieve this by setting the transformed values for repeated observations as the average of the corresponding back-to-back ranking numbers, unless the repeated values equal the largest observation $X_{[n]}$ in which case these repeated observations get transformed values equal to 1. Formally, if our sample of n observations drawn from $\{X\}_t$ includes repeated values, then (3.2) becomes

$$F_n(X_j) = \begin{cases} \frac{\beta_{[r]}}{n} & \text{for } X_{[r]} \leq X_t < X_{[r+1]}, r = 1, 2, \dots, n-1 \\ 1 & \text{for } X_t \geq X_{[n]} \end{cases}$$

where β_r takes values depending on whether the current observation (r th observation in the ordered sample) is unique or repeated. If the observation is unique, then $\beta_r = r$. If the observation is repeated, then β_r equals average of the ranking numbers of repeated observations.

As an example, imagine that two observations in the ordered sample with ranking numbers $r-1$, $r < n$ are equal. Then

$$\beta_{r-1} = \beta_r = \frac{(r-1) + r}{2}$$

On the other hand, if the two repeated values equal the maximum value of the sample, i.e. $r = n$, then

$$\beta_{r-1} = \beta_r = 1$$

As in the case of non-repeated values, X_j are projected into transformed values z_j via equation (3.3).

In Holló et al. (2012, p. 15) authors note that at this point we still haven't introduced the "real-time" character of the stress index. To feature this property, we will apply the ECDF transformation recursively for new observations drawn from $\{X\}_t$. Precisely, the non-recursive transformation in (3.3) applies to all first n observations which can be thought of as an "initial" sample. Imagine that, in addition to the initial sample of n observations, we draw $N - n$ more observations from $\{X\}_t$. All these subsequent observations are transformed via ECDF with one new observation added at a time. Assuming again that

³This special case wasn't clearly distinguished either in Holló et al. (2012) nor Schüler et al. (2015).

there are no repeated values, for $k \in [1, N - n]$ define the updated empirical ECDF as

$$F_{n+k}(X_{n+k}) = \begin{cases} \frac{r}{n+k} & \text{for } X_{[r]} \leq X_{n+k} < X_{[r+1]}, r = 1, 2, \dots, n-1, \dots, n+k-1 \\ 1 & \text{for } X_{n+k} \geq X_{[n+k]} \end{cases} \quad (3.4)$$

where $n + N$ is the number of observations in the full sample. Now for each $k \in [1, N - n]$ we project X_{n+k} into a transformed variable z_{n+k} according to the rule

$$z_{n+k} = F_{n+k}(X_{n+k}) \quad (3.5)$$

Repeated values are handled exactly the same way as in the pre-sample case.

In conclusion, when we normalize the four financial cycle series $\{I_i\}_t$, $i = 1, \dots, 4$, using the method described in this subsection, we obtain four stress factor series $\{z_i\}_t$, $i = 1, \dots, 4$ which will be used in the next subsection.

3.2.3 Aggregation of variables

After pre-multiplication and normalization of the financial cycle variables we are ready to aggregate them into a composite stress indicator. The aggregation method is a slight modification of the one used in Holló et al. (2012), and relies on time-varying weights assigned to variables. The weights are determined via *exponentially weighted moving averages* (EWMA) of the correlations between individual stress factors.

Formally, let us denote the resulting composite stress index series as $\{\psi\}_t$. Then the stress index value at given time t is given by

$$\psi_t = (\mathbf{1}' C_t \mathbf{1})^{-1} \cdot \mathbf{1}' C_t Z_t$$

where

$$Z_t = [z_{1,t}, \dots, z_{S,t}]'$$

is a vector of $S = 4$ stress factors at time t , and $\mathbf{1}$ is a vector of ones. C_t denotes the correlation coefficient matrix at time t :

$$C_t = \begin{bmatrix} \rho_{11,t} & \rho_{12,t} & \dots & \rho_{1S,t} \\ \rho_{21,t} & \rho_{22,t} & \dots & \rho_{2S,t} \\ \vdots & \vdots & \dots & \vdots \\ \rho_{S1,t} & \rho_{S2,t} & \dots & \rho_{SS,t} \end{bmatrix} \quad (3.6)$$

Correlation between stress factors z_i and z_j , ρ_{ij} , is given by

$$\rho_{ij} = \frac{\sigma_{ij,t}}{\sqrt{\sigma_{ii,t} \sigma_{jj,t}}}, \quad i, j = 1, \dots, 4, \quad ,$$

where σ_{ij} denotes the covariance between z_i and z_j , i.e.

$$\begin{aligned} \sigma_{ij,t} &\equiv \text{Cov}_t(z_{i,t+1}, z_{j,t+1}) \\ \sigma_{ii,t}^2 &\equiv \text{Cov}_t(z_{i,t+1}, z_{i,t+1}) = \text{Var}_t(z_{i,t+1}) \end{aligned}$$

As mentioned above, we assume that covariances are estimated recursively on the basis of EWMA dynamics, which means that $\forall t^4$

$$\begin{aligned} \sigma_{ij,t} &= \lambda \sigma_{ij,t-1} + (1 - \lambda) \left(z_{i,t} - \frac{1}{2} \right) \left(z_{j,t} - \frac{1}{2} \right) \quad \text{for } i \neq j \\ \sigma_{ii,t} &= \lambda \sigma_{ii,t-1} + (1 - \lambda) \left(z_{i,t} - \frac{1}{2} \right)^2 \end{aligned}$$

The estimated covariance for current period is thus a linear combination of past estimated covariance and current values of the two stress factors. Covariances are initialized using first 8 observations for each variable. The decay parameter λ is set to $\lambda = 0.89$. As a final note, correlations appearing in (3.6) are restricted such that negative correlations are forced to zero. That is, whenever $\rho_{ij,t} < 0$, we set $\rho_{ij,t} = 0$. At first glance this seems to be a rather technical restriction, but Schüler et al. (2015, p. 12) argue that imposing the restriction ensures that the CFC emphasizes "directional developments of systemic nature".

3.3 Power Cohesion and endogenous frequency band

The third phase in construction of the CFC deals with identifying a frequency band that will be used in filtering the composite stress index ψ . The identification of this band is conducted using the so-called *Power Cohesion* (PCoh) metric introduced in Schüler et al. (2015). In essence, PCoh is a function whose values correspond to average of normalized cross-spectral densities of the financial cycle variables. The higher the value of PCoh at given frequency, the more co-movement variables exhibit at that frequency. The frequency band is obtained by extracting a range of frequencies capturing the most mass under the

⁴Since stress factors lie in interval $(0, 1]$, subtracting the theoretical median $\frac{1}{2}$ corresponds to demeaning. We notice further that $\sigma_{ii} = \sigma_i^2$ (variance = volatility to the second power).

PCoh curve. In more detail, PCoh at angular frequency ω is given by (Schüler et al., 2015, p. 6)

$$PCoh_I(\omega) \equiv \frac{1}{S(S-1)} \sum_{i \neq j} \frac{|h_{ij}(\omega)|}{\sigma_i \sigma_j} \quad (3.7)$$

where $i, j \in \{1, \dots, S\}$, $\omega \in [-\pi, \pi]$, and $h_{ij}(\omega)$ denotes the cross-spectral density of series $\{I_i\}_t$ and $\{I_j\}_t$. Further, σ_i denotes the standard deviation of $\{I_i\}_t$.

We estimate the cross-spectral densities as laid out in sections 2.4.2 and 2.4.3. That is, we will use the Blackman-Tukey estimator in conjunction with Parzen lag window. These choices are made to match the selections of Schüler et al. (2015) in order to derive comparable results. For ease of reference, we reproduce the Blackman-Tukey estimator for the cross-spectral density (equation 2.31)

$$\hat{h}_{ij}^{BT}(\omega) = \frac{1}{2\pi} \sum_{r=-(N-1)}^{N-1} \lambda(r) \hat{\gamma}_{ij}(r) e^{-i\omega r} \quad (3.8)$$

As noted in our discussion about the consistent estimation of spectral densities, the choice of truncation parameter $M = 2N + 1$ is important as it specifies a trade-off between variance and bias of the estimator. Following the choice made in Schüler et al. (2015, p. 10), in our work we also set $M = \lceil 5\sqrt{T} \rceil$. Schüler et al. (2015, p. 10) argue that this choice is made in order to obtain rather unbiased estimates at the cost of increased variance. As an example, for Germany we have in total 185 observations, which results in $M = 69$.

In order to calculate the estimator in (3.8) we rely on *Matlab's Fast Fourier algorithm*. Recalling our discussion in section 2.2.2 about calculating FFTs, we first circularly shift the term $\lambda(r)\hat{\gamma}_{ij}(r)$ in (3.8) by N steps to the right, and then feed the result to the DFT algorithm (2.15).⁵ In section A.6 of the Appendix we provide a Matlab code snippet for calculating equation (3.8). Once we have estimated the cross-spectral densities, the frequency band containing most of the co-movement between variables is determined by the following optimization problem:⁶

⁵In order to conserve power correctly, we need to scale the output by $\frac{1}{N}$. Although we pay extra attention to right scaling of the DFT, in our setting this is actually not crucial as the resulting frequency band is identified by the relative shapes of the estimated cross-spectral densities rather than their absolute values.

⁶Note that in Schüler et al., 2015 equation 17 the problem was written as

$$\min_{\omega_2, \omega_1} \frac{\int_{\omega_1}^{\omega_2} PCoh_X(\omega) d\omega}{\int_0^{\pi} PCoh_X(\omega) d\omega} \geq p \quad ,$$

which is somewhat misleading since the point is to minimize the distance $\omega_2 - \omega_1$.

$$\begin{aligned}
 & \min_{\omega_2, \omega_1} \omega_2 - \omega_1 & (3.9) \\
 \text{s.t.} & \frac{\int_{\omega_1}^{\omega_2} PCoh_I(\omega) d\omega}{\int_0^{\omega_{max}} PCoh_I(\omega) d\omega} \geq p
 \end{aligned}$$

where $p \in [0, 1]$ indicates a ratio of co-movement we want to capture from the frequency interval $[0, \omega_{max}]$. We set $\omega_{max} = \frac{2\pi}{5}$, meaning $\omega_1, \omega_2 \in [0, \frac{2\pi}{5}]$ such that $\omega_2 \geq \omega_1$.⁷ Restricting ω_1 and ω_2 to interval $[0, \frac{2\pi}{5}]$ essentially means that cycles with periods below 5 quarters (or equivalently above angular frequency $\frac{2\pi}{5}$) are excluded from the frequency band by assumption. See Schüler et al. (2015) page 11 for discussion about this assumption.

3.4 Filtering the stress index

In the fourth and last phase we use the band-pass filter championed by Cristiano and Fitzgerald (2003) to smooth the stress index.⁸ The idea of a band-pass filter is to let only frequencies within a certain band to pass, and filter out components operating at all other frequencies. The filter comes in many forms which, even at best, are only approximations of the optimal band-pass filter. We will adopt the version that authors call *Random Walk Filter*, which would be optimal band-pass filter if the data used was generated by a random walk. However, Cristiano and Fitzgerald (2003) note that the differences between the Random Walk filter and more advanced filters are typically small, so often Random Walk filter is a good choice due to its character of being fairly parsimonious. Schüler et al. (2015, p. 11) also use this version by an argument that they want to keep the distorting effects of the filter to minimum. Section A.5 in Appendix offers a short formal treatment of the Random Walk filter.

As the band-pass filter is a two-sided filter, it suffers from end-point problems in the sense that values close to the edges of a finite sample are poorly estimated. As an attempt to remedy this problem, Schüler et al. (2015) forecast the stress index 10 years forward using a fitted AR(1) model. They then filter the stress index (with forecasts) using the band-pass filter, and finally cut observations from the end of the filtered series

⁷Schüler et al., 2015 set $\omega_{max} = \pi$, which means that they take the co-movement across all possible frequencies into account in the denominator. This might not be desirable, however; when $\omega_{max} = \pi$, for PCoh functions that have a lot of mass at frequencies above the threshold ω_2 we often don't find a portion $\int_{\omega_1}^{\omega_2} PCoh_I(\omega) d\omega$ that is greater than $p * \int_0^{\pi} PCoh_I(\omega) d\omega$. In this case we cannot determine the frequency interval endogenously using PCoh. We thus have a reason to suspect that there is a typo in the original paper, and for this reason in this thesis we set $\omega_{max} = \frac{2\pi}{5}$.

⁸Codes are available at Federal Reserve Bank Atlanta's homepage <https://www.frbatlanta.org/cqer/research/bpf.aspx>

by an amount corresponding to the amount of forecasted values. We employ the same procedure, however we use a shorter forecast horizon of 2 years as instructed by Cristiano and Fitzgerald (2003) in the code file accompanying the paper (see footnote 8).

We have now derived our financial cycle proxy. In the next chapter we will scrutinize how the obtained CFCs perform in early warning exercises.

Chapter 4

Empirical Results

In this chapter we present our empirical results. First, we will give an overview of the obtained CFCs as well as the periodicity (or equivalently, frequency) bands. Secondly, we will present results from two early-warning exercises to scrutinize how well our financial cycle proxy explains known periods of banking crises and financial stress. Lastly, we will comment how our results compare with ones obtained by Schüler et al. (2015).

4.1 Visualization of Composite Financial Cycles

Figure 4.1 summarizes the obtained CFC as well as the unfiltered stress index ψ for each country in our sample. Shaded areas represent known periods of banking crises as defined by Laeven and Valencia (2012).¹ Visual inspection reveals that for most parts the CFCs fulfil the desired criteria, in particular that a) cycles are smooth compared to the unfiltered stress index ψ , indicating a parsimonious selection of frequencies, and b) crisis periods tend to follow peaks in the CFC with a few years lag. In most cases peaks in the cycle preceding crisis periods are also among the highest for a given country, implying that periods of rapid growth in credit, house prices, stocks, and (inversely) bond yields tend to build up macro-financial imbalances which can result in costly banking/financial crises.

However, it is important to note that not every cycle peak is followed by a crisis. There are many possible reasons for this. First, some local peaks are fairly flat which indicates that the build-up in macro-financial sector has been fairly short-lived. Second, banking crises can be defined in many ways, and hence different sources locate crises in different points in time. The Laeven and Valencia (2012) database alerts for crisis only when two rather strict conditions are met, resulting in fewer crises periods than in alternative crisis databases such as Babecký et al. (2012) and Detken et al. (2014). Third, it is possible

¹We use this particular dataset to indicate banking crises periods as it is the most common one used in related literature. See Appendix A.8 for more details about the crisis dataset.

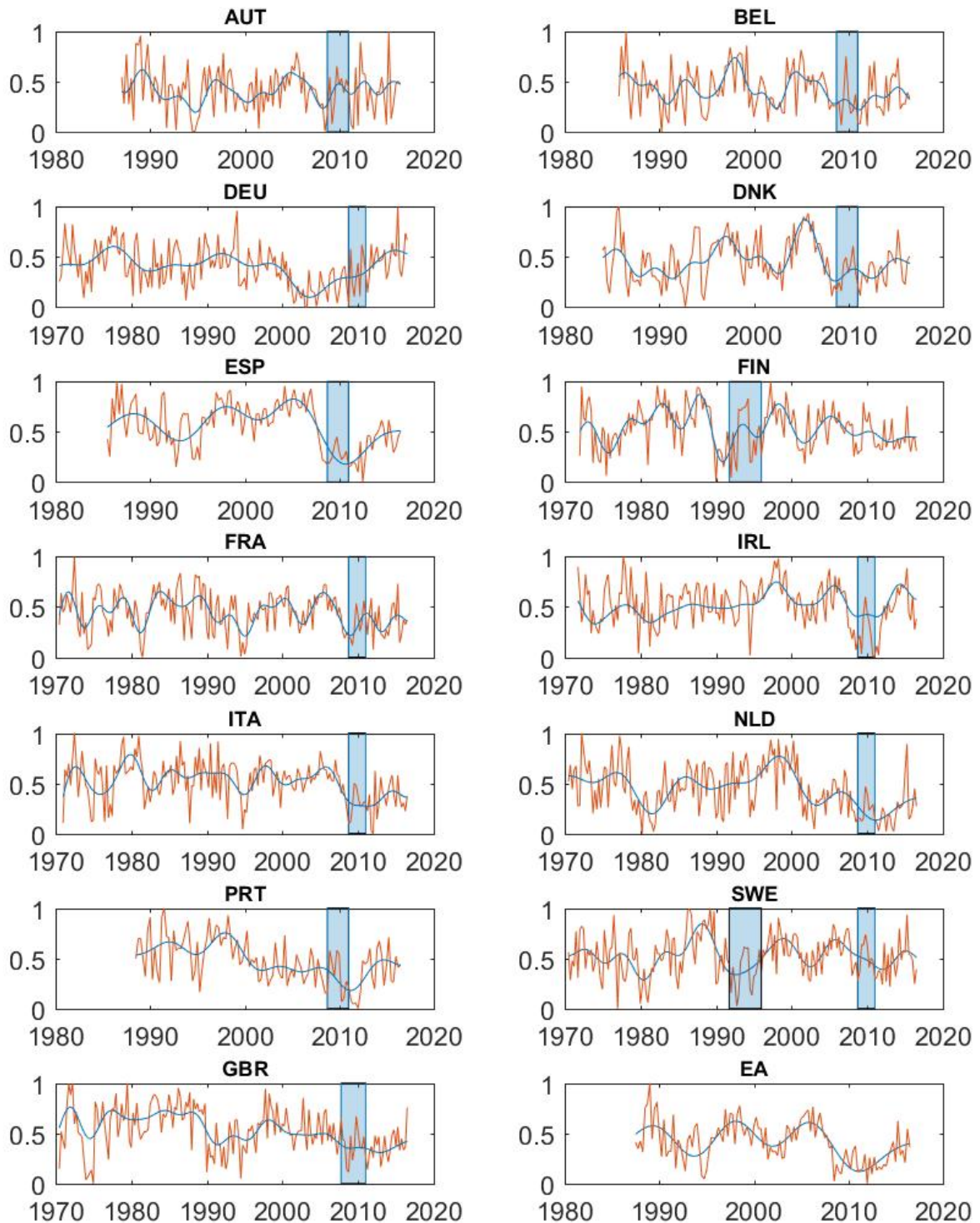


Figure 4.1: Composite Financial Cycles for sample countries. The CFCs are derived using all available data. Blue lines represent the CFC and orange lines unfiltered stress index ψ . The y-axis is by construction restricted to range $(0, 1]$. Shaded areas represent crisis periods identified by Laeven and Valencia (2012).

that crises are prevented by proactive regulatory measures. Lastly, and perhaps most realistically, not all build-ups escalate into crises by sheer randomness.

In order to compactly summarize the information from individual cycles, we calculate the deviations of the CFCs from their own historical mean and plot this range over time. The resulting graph is shown in Figure 4.2, accompanied by the deviation series for Germany, Spain, Italy, and the euro area aggregate. We see that there was a consistent and even-timed build-up in the macro-financial sector across countries before the "dot-com" bubble. Before the financial crisis of 2007-2008 the maximum deviation was even higher, although not in all countries (especially in Germany) was the cycle above its historical mean value. This would reinforce the popular story that although there were imbalances brewing in some European countries, the ultimate shock that led to the financial crisis was exogenous, ignited by the housing market collapse in the United States. During the onset of the euro area debt crisis cycles in all sample countries were below their historical mean but have rebounded since. The recovery has not been totally uniform, however, as in Q2 of 2016 some countries - namely Italy and Spain - were still below the historical mean. Euro area aggregate was just about to reach its mean level.

As explained in detail in Chapter 3, a band-pass filter is used on stress index ψ to obtain the CFC. Thus, the periodicity band (or equivalently frequency band) used in filtering process plays an important role in the formation of the CFC. The longer the periods allowed to pass through the filter, the smoother the CFC becomes, and vice versa. In Table 4.1 we present the periodicity bands identified for our sample countries. Figure A.1 in Appendix plots the Power Cohesion graphs through which the periodicity bands are identified.

Several important characteristics become evident from these results. First, peaks in Power Cohesions are located at period lengths above 8 years for all countries except Austria, where the peak is right about at 8 year mark. We hence conclude that financial cycles are rather long, with most important cyclicity taking place at periods above 8 years. Secondly, we identify very large values for the upper bounds of the periodicity bands (or equivalently, very small values for the lower ends of the frequency bands) uniformly across countries. As these periods are much greater than the length of the sample in our disposal, we can expect them to be poorly estimated and should thus be handled with some degree of doubt. However, it turns out that the long end of the periodicity band is of little practical importance. Schüler et al. (2015, p. 11) explain that the results for the case where the maximum period length is forced to 50 years (the approximate length of the so-called *Kondratiev waves*) are almost equivalent to the unrestricted case. This makes intuitive sense as cycles much longer than the available sample data are far too smooth to be of any relevance for empirical analysis. What matters most for the shape of the CFC is

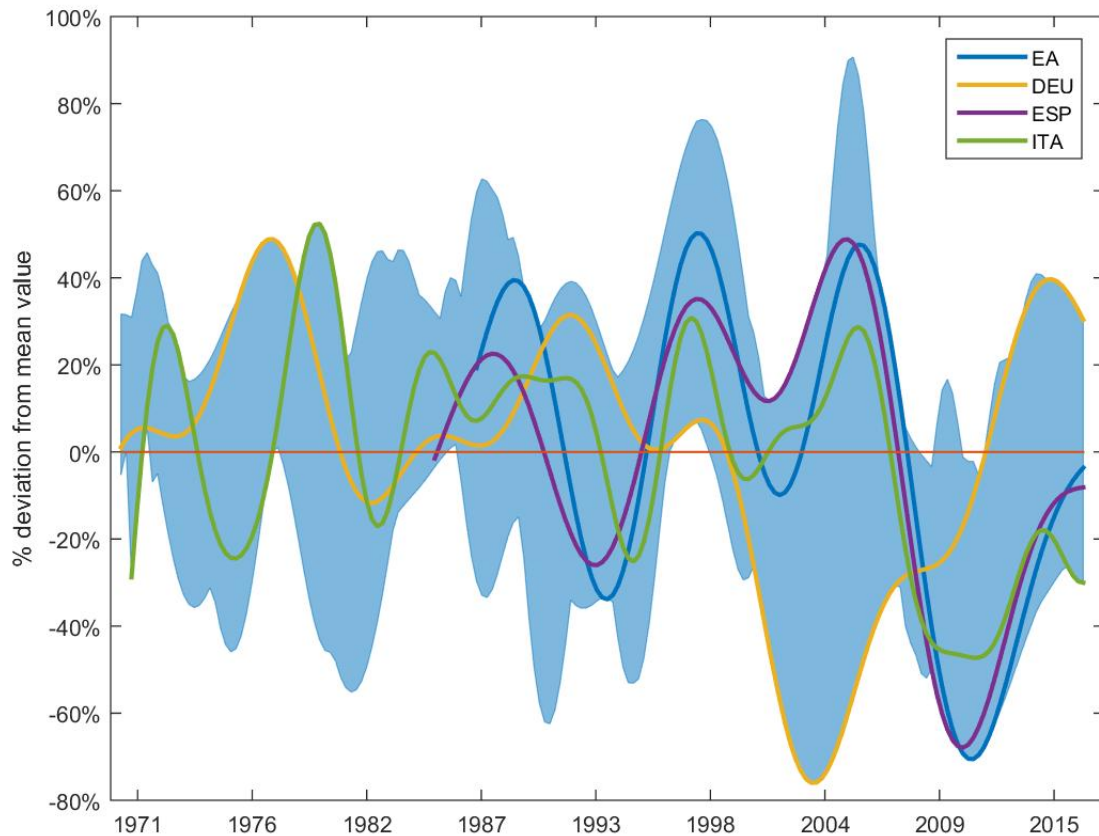


Figure 4.2: Range of deviations of CFCs from their historical mean values, plotted with deviation of euro area aggregate CFC from its historical mean. Total time range is 1970Q1-2016Q2. High values indicate large deviations from the mean value and thus possible building imbalances.

the lower end of the periodicity band. This relates to the third observation, namely that there are clear heterogeneities in the lower periods across countries. For Germany and Spain (as well as the euro area aggregate) the lower ends of the periodicity bands are fairly high compared to other countries, which explains the higher degree of smoothness of the CFC for these countries. This would suggest that in Germany and Spain financial cycles tend to be longer lasting than in other sample countries.

Country	Periodicity band
AUT	2.5 - 159.8
BEL	2.8 - 162.3
DEU	6.9 - ∞
DNK	3.5 - ∞
ESP	6.5 - 162.8
FIN	4.2 - ∞
FRA	3.5 - ∞
IRL	3.6 - 190.3
ITA	4.3 - ∞
NLD	6.4 - ∞
PRT	4.5 - ∞
SWE	4.5 - ∞
GBR	4.2 - 192.8
Mean	4.4 - ∞
Median	4.2 - ∞
EA	6.9 - 158.8

Table 4.1: Ranges of identified periodicity bands measured in years. EA is excluded from mean and median. Corresponding frequency band end points are obtained via formula $\omega = 2\pi\frac{1}{T}$, where T is the period length in quarters.

4.2 Early warning properties

In this section we investigate results from two early-warning exercises. First, we perform a pooled logit early warning regression typical in the related literature. Second, we investigate the CFC for Finland in more detail by comparing it to a market-based stress index.

4.2.1 Pooled logit early warning regression

Beside the visual inspection of the series, we would like to quantify the extent to which the CFCs are helpful in detecting costly banking/financial crises. We do this by following typical early warning literature, which includes works such as Frankel and Rose (1996), Demirgüç-Kunt and Detragiache (2000), Schularick and Taylor (2012), Alessi and Detken (2011), as well as Lo Duca and Peltonen (2013). In essence, we perform a pooled logit regression where we explain known financial crisis periods with our financial cycle proxy.

Using the estimates obtained from this regression we can construct model-implied crisis probabilities over time. We then compare these crisis probabilities to actual crisis periods and derive evaluation metrics such as *area under receiver operating characteristic curve* (AUROC) and *usefulness for policymaker* (or *usefulness* for short), which indicate whether the CFC is a good measure for early warning purposes. As the end-point problems arising from the filtering process might be of real importance, we consider two versions of the CFC: a) CFC derived on full sample, i.e. estimated using all available data, and b) CFC where filtering is conducted on expanding fashion.²

In formal terms, the early warning regression is performed as follows. First we identify crisis dummy series for each of the countries within the intervals given in Table 3.2. We will denote these series as $\{y\}_t$. For example, if a country k faced a crisis in certain period t , then $y_{k,t} = 1$, and if there was no crisis, $y_{k,t} = 0$. As the aim is to detect costly banking crises *in advance*, instead of explaining the actual crises periods we want to explain some time period preceding the crises. We call this time period *vulnerability horizon*. Thus, we create transformed crisis dummy series $\{\hat{y}\}_t$ where values 1 indicate that there will be a crisis in a given vulnerability horizon, and values 0 that there is no crisis in a given horizon. As we want to be able to detect crises well in advance, we set our baseline vulnerability horizon to be 2.5-4 years, or 10-16 quarters. We also test for another vulnerability horizon of 1-3 years, or 4-12 quarters. As an example with quarterly observations and the baseline vulnerability horizon, if we know that $y_{k,t} = 1$ and otherwise zero, then we also have that $\hat{y}_{k,t-16}, \hat{y}_{k,t-15}, \dots, \hat{y}_{k,t-10}$ will have value 1 and otherwise value zero.

Next we run a pooled logit regressions using all available data from time period 1970Q1-2016Q2.³ We use the obtained CFCs as the explanatory variable, including intercept.⁴ The explained variable is \hat{y} . In order to treat possible biases arising during crisis periods (see e.g. Behn et al., 2013 and Bussière and Fratzscher, 2006), we remove those periods from the sample that actually witnessed a crisis (i.e. periods where $y_t = 1$) as well as periods 6 quarters after the witnessed crisis (i.e. periods $t + 1, \dots, t + 6$ after t where $y_t = 1$). Furthermore, we also drop observations that are left between the vulnerability

²CFC derived on expanding fashion is how Schüler et al. (2015) present their early warning regression results. "Expanding" here means that the band-pass filtering is conducted adding one new observation at the time. It does *not* mean that the ECDF transformation or estimation of spectral densities would be conducted on expanding fashion, something which is not clearly stated in the original reference.

³Using country fixed-effects is not possible due to lack of observations. For discussion on the appropriateness of a pooled approach, see e.g. Demirgüç-Kunt and Detragiache (2000). Further, we exclude the euro area aggregate from early warning regressions as it is not included in the crisis dataset.

⁴As is evident from Table 3.2, for some countries the time period for which the CFC is available is shorter than that of 1970Q1-2016Q2. This means that for some countries we have less observations in the pooled sample. One possibility would be to truncate sample lengths so that each country would have the same sample length, but we avoid doing so as it would decrease our sample size too much.

horizon and start of the crisis as these values would also introduce an unwanted bias. Pooled logistics regression with intercept and one explanatory variable reads

$$p \equiv P(\hat{y} = 1) = \frac{e^{\beta_0 + X\beta_1}}{1 + e^{\beta_0 + X\beta_1}} ,$$

where X contains pooled CFC values. After obtaining estimates $\hat{\beta}_0$ for the intercept and $\hat{\beta}_1$ for the CFC, we can use them to construct model implied crisis probability series over time for each country k as

$$\hat{p}_{k,t} = \frac{e^{\hat{\beta}_0 + CFC_{k,t}\hat{\beta}_1}}{1 + e^{\hat{\beta}_0 + CFC_{k,t}\hat{\beta}_1}} ,$$

where $CFC_{k,t}$ indicates the value of the financial cycle proxy for country k at time t . We obtain binary crisis predictions by comparing the implied crisis probability to some threshold level τ :

$$P_{k,t}(\tau) = \begin{cases} 1 & \text{if } p_{k,t} > \tau \\ 0 & \text{if } p_{k,t} \leq \tau \end{cases}$$

That is, if the implied crisis probability for a given period t exceeds τ , then $P_{k,t} = 1$ and an alert for crisis will be raised.

From the binary predictions we can calculate usual early warning signalling statistics. Specifically, we can derive the so-called *confusion matrix* observations true positive (TP), true negative (TN), false positive (FP), and false negative (FN) as laid out in table 4.2:

	$P_{t,k}(\tau) = 1$	$P_{t,k}(\tau) = 0$
$\hat{y}_{t,k} = 1$	$TP(\tau)$: Correct alarm	$FN(\tau)$: Missed crisis
$\hat{y}_{t,k} = 0$	$FP(\tau)$: False alarm	$TN(\tau)$: Correctly no alarm

Table 4.2: Confusion matrix.

Further, confusion matrix values allow us to calculate *true positive rate* and *false positive rate*, defined as

$$TPR(\tau) = \frac{TP(\tau)}{TP(\tau) + FN(\tau)}$$

$$FPR(\tau) = \frac{FP(\tau)}{FP(\tau) + TN(\tau)}$$

Now imagine we were to plot $TPR(\tau)$ and $FPR(\tau)$ for different values τ in a FPR-TPR plane. The resulting curve goes by the name *receiver operating characteristic* (ROC), and the area under the ROC is referred to as AUROC. AUROC exhibits how well our model explains banking crises over all values τ . The bigger the AUROC, the higher the ratio $\frac{TPR}{FPR}$ on average.

Sometimes AUROC alone might not be the best metric in evaluating early warning properties. For example, there might be just a few values of τ that produce a high $\frac{TPR}{FPR}$ ratio, in which case AUROC will not generally be high. To overcome this possible challenge we introduce the (*absolute*) *usefulness* metric championed by Alessi and Detken (2011). To this end, we first define the *loss function* $L(\tau)$ as

$$L(\tau) \equiv \theta \frac{FN(\tau)}{TP(\tau) + FN(\tau)} + (1 - \theta) \frac{FP(\tau)}{FP(\tau) + TN(\tau)} \quad ,$$

where " θ is the parameter revealing the policy maker's relative risk aversion between type I and type II errors" (Alessi and Detken, 2011, p. 523). When θ equals 0.5 the policy maker treats both type I and II errors as equally bad outcomes. If the policy maker is willing to accept more false positives in return of less type II errors (false negatives) and hence more true positives, she will set $0 < \theta < 0.5$, and vice versa. In turn, (*absolute*) usefulness is defined as

$$U_a = \min\{\theta, 1 - \theta\} - L$$

As suggested by Sarlin (2013), we can present the idea of usefulness in a slightly different way. Namely, we can introduce a ratio called *relative usefulness* which states how well we fair against a perfect model where loss equals zero. Relative usefulness is thus defined by⁵

$$U_r = \frac{U_a}{\min(\theta, 1 - \theta)}$$

Table 4.3 summarizes results from the early warning regressions. We see that, in the vulnerability horizon of 10-16 quarters, our financial cycle proxy, derived both on full and expanding samples (denoted as " CFC^a full" and " CFC^a exp.", respectively), performs well in detecting banking crises. AUROCs for the full and expanding sample CFCs are

⁵Sarlin (2013) extended the loss function of Alessi and Detken (2011) to explicitly take into account unconditional sample crisis probabilities in order to correct for biases arising from the fact that tranquil times are much more common than crises periods. However, Alessi and Detken (2014) defend their less complicated loss function by arguing that introducing relative sample sizes is "not robust to minor changes in preferences or in the probability of crises". As we wish to keep our analysis as parsimonious as possible, we opt not to introduce unconditional sample probabilities into the loss function.

Variables	Horizon 4-12 quarters				Horizon 10-16 quarters							
	(i)	(ii)	(iii)	(iv)	(v)	(vi)	(vii)	(viii)	(ix)	(x)	(xi)	(xii)
Intercept	-2.9***	-2.9***	-2.5***	-3.2***	-3.6***	-5.2***	-3.2***	-3.2***	-5.5***	-4.9***	-6.2***	-5.5***
I_1	19.0***	18.7***					12.5**	12.5**				
I_2	-2.5	-0.1					9.0**	8.8**				
I_3	4.1***	3.1***					4.6**	5.0***				
I_4	0.9***						-0.0					
CFC^a full			0.0						5.2***			
CFC^a exp.				2.7***						4.6***		
CFC^b full					2.1***						6.3***	
CFC^b exp.						5.4***						5.7***
AUROC	0.60	0.61	0.50	0.52	0.60	0.65	0.45	0.66	0.69	0.68	0.76	0.75
U_r	0.22	0.18	0	0.10	0.18	0.28	0	0.28	0.30	0.26	0.40	0.40
Obs	1637	1637	1637	1325	1652	1340	1501	1501	1501	1189	1516	1204

Table 4.3: Pooled logit early warning regression results for individual variables and composite financial cycle, derived both on full and expanding samples. CFC^a is constructed using all 4 financial cycle variables, in CFC^b bond yields are excluded. $I_i, i = 1 \dots 4$ refer to series in (3.1). Maximum time span of data sample is 1970Q1 - 2016Q2, although for some countries series are shorter due to data availability issues. Explained variable is a dummy series where values 1 indicate Laeven and Valencia (2012) banking crises for a given horizon in advance. Relative usefulness is derived using $\theta = 0.5$. Asterixes indicate statistical significance at certain levels: * = 10%, ** = 5%, and *** = 1%.

0.69 and 0.68, respectively, indicating a clear improvement over a coin-toss situation of $AUROC = 0.5$. Furthermore, relative usefulness values are 0.30 and 0.26, respectively, meaning that we achieve around 30% success compared to a perfect model. However, for the vulnerability horizon closer to the onset of crises (4-12 quarters) we don't find any particular early warning success. This clearly stands in contradiction with findings by Schüler et al. (2015) and will be discussed in more detail in section 4.3.

Extending the analysis beyond to that reported in Schüler et al. (2015), we highlight the role of bond yields in our early warning setting. Columns (i) and (vii) show the results from early warning regressions where we, instead of the CFC, use series $I_i, i = 1 \dots 4$ from (3.1) as explanatory variables. Comparing these two columns to columns (ii) and (viii), respectively, excluding bond yields from the explanatory variables improves the performance of the model in both vulnerability horizons. In particular, for vulnerability horizon of 10-16 quarters the improvement is considerable. Thus, we have reason to believe that including bond yields in the CFC might erode its early warning performance. Running the analysis excluding bond yields from the CFC – shown as CFC^b in the table – confirms this result: AUROC and usefulness exhibit clear improvements in both vulnerability horizons. At vulnerability horizon of 10-16 quarters, we derive AUROC values 0.76/0.75 and relative usefulness values 0.40/0.40 for full and expanding samples, respectively. Our results suggest that, at least as far as the early warning properties are concerned, bond yields should be excluded from the financial cycle proxy.

4.2.2 Comparison of CFC and Financial Stress Index for Finland

To further investigate the early warning properties of the CFC, we compare it to index-based measure of financial stress derived from daily market quotes. We reduce the analysis here to consider only Finland as we have the stress index data readily available through Bank of Finland's database link. Specifically, we employ the *Financial Stress Index* (FSI) for Finland as introduced in Huotari (2015). The FSI collects daily financial market data from several sectors and aggregates it into a composite indicator of financial stress.⁶ The FSI is essentially a Finnish version of the CISS calculated for the euro area by Holló et al. (2012).

Figure 4.3 presents the FSI plotted with both the CFC and the stress index ψ . Visual inspection of the upper graph reveals that peaks in the CFC tend to advance spikes in the FSI. Prior to periods where the FSI shoots up there is a local maximum in the CFC. Further, when the stress actually hits the economy, i.e. the FSI is at its local maximum, the CFC is already at the bottom of its cycle or approaching it. This relationship is reinforced

⁶The sectors are bond market, money market, foreign exchange market, equity market, and banking. See Huotari (2015) for more information.

by negative correlation (-0.2) between the stress index ψ and the FSI. In summary, we can confirm for Finland that the CFC can detect also periods of increased financial stress which do not necessarily lead to a full-blown crisis.

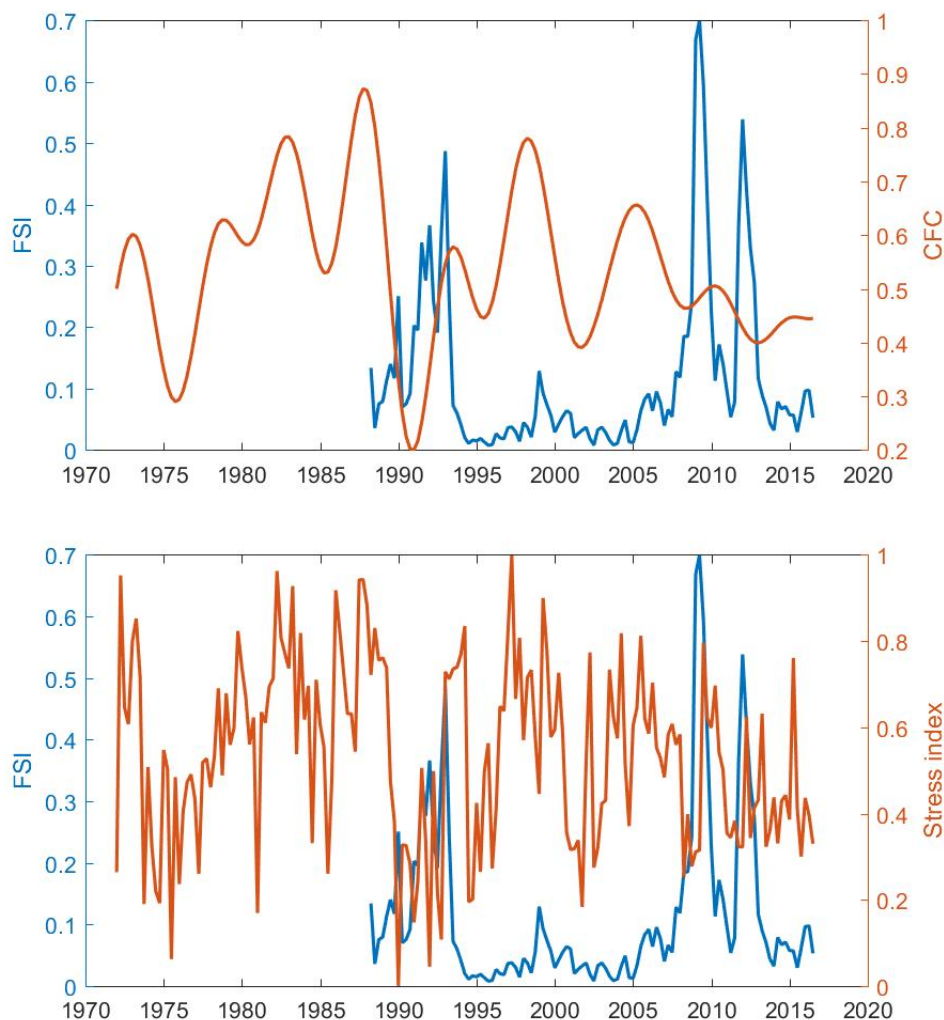


Figure 4.3: Financial Stress Index for Finland, calculated for interval 1988Q1-2016Q2 using "portfolio theoretic aggregation" method (Huotari, 2015), plotted with CFC and stress index ψ for Finland. Note that y-axes are adjusted slightly for comparison purposes.

4.3 Comparing results with Schüler et al. (2015)

To finish the chapter we briefly discuss how our results compare to conclusions originally presented in Schüler et al. (2015). To begin with, contrasting our table 4.1 to that of table 2 in the reference paper (Schüler et al., 2015, p. 19), our lower ends of the periodicity bands (i.e. higher ends of the frequency bands) are greater than in the reference paper. In our work mean and median of lower ends of the periodicity bands are 4.4 and 4.2 years, respectively, whereas in Schüler et al. (2015) they are 2.8 and 2.6 years, respectively. Further, in our work also the longer ends of the periodicity bands are greater than those in Schüler et al. (2015) (however, as discussed in section 4.1, this bears less importance). In summary, in this work we filter out shorter periodicity components which makes our cycles smoother than those of Schüler et al. (2015). The reason why we pick up longer periodicities is hard to pinpoint, but the fact that some of the data series - and especially their lengths - differ from those used in Schüler et al. (2015) can influence the identified frequency bands. Furthermore, the estimation of spectral densities is a very delegate process where only small parameter changes and/or coding differences may affect the results.

The fact that our cycles are smoother brings about two implications, one supporting the results in Schüler et al. (2015) and the other inflicting a contradiction. Despite slightly smoother curves found in our work, we can confirm the finding of the reference paper that lower ends of the periodicity bands for most countries (AUT, BEL, DNK, FIN, FRA, ITA, PRT, SWE, and GBR) are well below the 8 years suggested by earlier literature such as Drehmann et al. (2012). Further, as argued by the reference paper, we also find important heterogeneities across countries in the lower ends of the periodicity bands. As a contradictory consequence of smoother cycles, our CFC measure picks up warning signals earlier than that of Schüler et al. (2015). In particular, we find our CFC to be virtually of no use in vulnerability horizon of 4-12 quarters, whereas in the horizon of 10-16 quarters the CFC exhibits good early warning properties.⁷ However, this property is actually desirable as detecting crises more in advance offers policy makers extra time to prepare appropriate actions.

As a further point of comparison, Schüler et al. (2015) argue that bond yields co-move the least with other three variables included in the analysis, and are thus less relevant for the financial cycle proxy. We can bolster this finding from another point of view, namely on the basis of the early warning results, as we found that excluding bond yields from the financial cycle measure improves the early warning properties of the CFC substantially.

⁷In Schüler et al. (2015) authors considered a vulnerability horizon of 12-20 quarters instead of 10-16 quarters. We opted for 10-16 quarters as it yielded the best overall results in our setting.

Scrutinizing individual countries, there are a few occasions where the behaviour of the unfiltered stress index ψ as well as the CFC differ clearly from that reported in Schüler et al. (2015, p. 47-50). One particularly interesting case is Germany around the financial crisis of 2007-2008. Our results indicate Germany didn't experience much of a draw-down in macro-financial development during the financial crisis, nor a consistent build-up prior to the crisis. Schüler et al. (2015, p. 48), however, identify a local peak just before the financial crisis in both the CFC and the unfiltered stress index. This means that the dissimilarity to our result is not solely due to more smoothing than our frequency band indicates, but also due to differences in the levels of the stress index ψ . The reason for differing levels is again hard to pin-point, but a possible factor are differing house price series between our work and that of Schüler et al. (2015).

Chapter 5

Conclusion

In this thesis we provided a thorough construction of a financial cycle proxy for 13 European countries as well as for the euro area aggregate. We first motivated the need for such analysis and introduced essential parts from the theory of spectral analysis. Then, drawing inspiration from research conducted at the European Central Bank (Schüler et al., 2015), we aggregated four key macro-financial variables (credit, house prices, stock prices, and bond yields) into Composite Financial Cycle, or CFC for short, which summarizes the most important cyclical co-movement among the variables. Finally, we showcased how the obtained CFC fared in explaining known periods of financial crises, and compared these results with ones obtained by our main reference paper (Schüler et al., 2015).

Our findings are mostly in line with the reference paper. First, most important cyclical co-movement of the financial cycle takes place at periods above 8 years as indicated by the peaks of Power Cohesion function. Nevertheless, there exists relevant cyclicity also outside the period range of 8-30 years identified by earlier literature, and there seems to be important heterogeneities across countries at lower periods. Lastly, from the four key variables bond yield is the least important in construction of the CFC as it diminishes the resulting early warning properties. The greatest difference in our analysis compared to that of Schüler et al. (2015) is that our results emphasize longer periods (or lower frequencies) as the source of most important co-movements. This results in smoother cycles, which in turn translates to our CFCs detecting crisis periods more in advance than the CFCs presented in the main reference paper. This, however, is a desirable property as detecting crises more in advance leaves policy makers extra time to react to looming crises.

All in all, we identify a financial cycle proxy that suits well the desired properties. In particular, our CFC is rather smooth, implying a parsimonious selection of relevant frequencies. Further, the peaks in the CFC are associated with time periods of financial stress. We thus conclude that the CFC makes an useful addition to the macroprudential toolkit of central banks and academics alike.

Appendix A

A.1 Circular shift

Let $\{X\}_n$ be a signal where $n = 0, \dots, N - 1$. That is, the N values of signal $\{X\}_n$ can be represented as vector

$$X = [X_0, \dots, X_{N-1}]$$

Let notation $\langle k \rangle_N$ denote the remainder of division $\frac{k}{N}$ for non-negative integers k , i.e.

$$\langle k \rangle_N \equiv \text{rem}\left(\frac{k}{N}\right), k = 0, 1, \dots$$

For example, $\langle 5 \rangle_2 = 1$. For negative integers k the operation is defined in a slightly more complicated way:

$$\langle k \rangle_N \equiv \text{rem}\left(\frac{|N * \lceil \frac{k}{N} \rceil + k|}{N}\right), k = -1, -2, \dots$$

For example, $\langle -2 \rangle_5 = \text{rem}\left(\frac{5*1-2}{5}\right) = 3$ and $\langle -6 \rangle_5 = \text{rem}\left(\frac{5*2-6}{5}\right) = 4$. Evidently, $\langle k \rangle_N$ is a periodic function of k with period N (Selesnick, 2017, p. 5), that is

$$\langle k + hN \rangle_N = \langle k \rangle_N, h = 0, \pm 1, \pm 2, \dots$$

Let $X^{[-m]}$ denote a vector of circular shifted of values of X by m steps to the right, where n th observations is given by

$$X_n^{[-m]} \equiv X_{\langle n-m \rangle_N}$$

As an example, shifting X one step to the right yields

$$\begin{aligned}
 X_0^{[-1]} &= X_{\langle 0-1 \rangle_N} &= X_{\langle N-1 \rangle_N} &= X_{N-1} \\
 X_1^{[-1]} &= X_{\langle 1-1 \rangle_N} &&= X_0 \\
 X_2^{[-1]} &= X_{\langle 2-1 \rangle_N} &&= X_1 \\
 &\vdots && \\
 X_{N-2}^{[-1]} &= X_{\langle (N-2)-1 \rangle_N} &&= X_{N-3} \\
 X_{N-1}^{[-1]} &= X_{\langle (N-1)-1 \rangle_N} &&= X_{N-2}
 \end{aligned}$$

which means

$$X^{[-1]} = [X_{N-1}, X_1 \dots X_{N-2}]$$

Correspondingly, setting m negative corresponds to circularly shifting our vector to left. For example, for $m = -2$ we have

$$\begin{aligned}
 X_0^{[2]} &= X_{\langle 0+2 \rangle_N} &&= X_2 \\
 &\vdots && \\
 X_{N-3}^{[2]} &= X_{\langle (N-3)+2 \rangle_N} &&= X_{N-1} \\
 X_{N-2}^{[2]} &= X_{\langle (N-2)+2 \rangle_N} &&= X_0 \\
 X_{N-1}^{[2]} &= X_{\langle (N-1)+2 \rangle_N} = X_{\langle N+1 \rangle_N} &&= X_1
 \end{aligned}$$

which means

$$X^{[2]} = [X_2, \dots, X_{N-1}, X_0, X_1]$$

A.2 Raw series

Tables A.1 - A.4 below present information on the raw series introduced in Table 3.1.

A.3 Deflating nominal raw series

All series used in our analysis are measured in real terms. Series that are not originally reported in real terms (credit and stock prices) are deflated with corresponding consumer price index series as follows. Let t_0 denote the base time period. Then for series $\{x\}_t$, the deflated value \hat{x}_t at any period $t > t_0$ is given by

$$\hat{x}_t = x_t * \left(\frac{\text{CPI}_t}{\text{CPI}_{t_0}} \right)^{-1}$$

A.4 De-trending series

Credit, house prices, and stock prices are originally reported in either nominal or index values, and are transformed to log QoQ changes, i.e. percentage changes. Bond yields are originally reported as percentage points and are transformed to QoQ percentage point changes. Formally, let $\{x_i\}_t$, $i = 1, 2, 3$, denote raw series credit, house prices, and stocks, respectively. We obtain the de-trended values $\{\Delta x_i\}_t$, $i = 1, 2, 3$, for every t as

$$\Delta x_{i,t} = \ln\left(\frac{x_{i,t}}{x_{i,t-1}}\right) \approx \frac{x_{i,t}}{x_{i,t-1}} - 1 = \frac{x_{i,t} - x_{i,t-1}}{x_{i,t-1}} = \text{"QoQ percentage change"}$$

Now let $\{x_4\}_t$ denote the raw series for bond yield. De-trended values for every t are given by

$$\Delta x_{4,t} = x_{4,t} - x_{4,t-1} = \text{"QoQ percentage point change"}$$

Credit to non-financial private sector						
Country	Description	Original unit	Time-span	Original frequency	(Dis-) aggregation	Source
AUT	Credit to non-financial private sector, ex. trade credit, not seasonally adjusted	Euro, bil.	1970Q1-2016Q2	Quarterly	-	BIS Credit Statistics, DBSONline
BEL	— " —	— " —	1970Q4-2016Q2	— " —	-	— " —
DEU	— " —	— " —	1970Q1-2016Q2	— " —	-	— " —
DNK	— " —	Danish Krone, bil.	1970Q1-2016Q2	— " —	-	— " —
ESP	— " —	Euro, bil.	1970Q1-2016Q2	— " —	-	— " —
FIN	— " —	— " —	1970Q4-2016Q2	— " —	-	— " —
FRA	— " —	— " —	1970Q1-2016Q2	— " —	-	— " —
GBR	— " —	Pound sterling, bil.	1970Q1-2016Q2	— " —	-	— " —
IRL	— " —	— " —	1970Q4-2016Q1	— " —	-	— " —
ITA	— " —	Euro, bil.	1970Q1-2016Q2	— " —	-	— " —
NLD	— " —	— " —	1970Q1-2016Q2	— " —	-	— " —
PRT	— " —	— " —	1970Q1-2016Q2	— " —	-	— " —
SWE	— " —	Swedish Krona, bil.	1970Q1-2016Q2	— " —	-	— " —
EA	Loans (stock) to households + non-financial corporations by MFIs excluding eurosystem	Euro, mil.	1980Q1-2016Q2	— " —	-	ECB SDW Balance Sheet Items

Table A.1: Raw series credit.

Residential property prices						
Country	Description	Original unit	Time-span	Original frequency	(Dis-) aggregation	Source
AUT	Residential property prices, new and existing dwellings, whole country, neither SA nor WA	Index 2007=100	1986Q3-2016Q2	Quarterly	-	ECB SDW Residential Property Price Index Statistics
BEL	Residential property prices, long series, NSA	Index 1995=100	1970Q1-2016Q2	— " —	-	BIS Residential Prices Statistics, DBSONline
DEU	— " —	— " —	1970Q1-2016Q2	— " —	-	— " —
DNK	— " —	— " —	1970Q1-2016Q2	— " —	-	— " —
ESP	— " —	— " —	1971Q1-2016Q2	— " —	-	— " —
FIN	— " —	— " —	1970Q1-2016Q2	— " —	-	— " —
FRA	— " —	— " —	1970Q1-2016Q2	— " —	-	— " —
GBR	— " —	— " —	1970Q1-2016Q2	— " —	-	— " —
IRL	— " —	— " —	1970Q4-2016Q1	— " —	-	— " —
ITA	— " —	— " —	1970Q3-2016Q2	— " —	-	— " —
NLD	— " —	— " —	1970Q1-2016Q2	— " —	-	— " —
PRT	Residential property prices, new and existing dwellings, whole country, neither SA nor WA	Index 2007=100	1988Q1-2016Q2	— " —	-	ECB SDW Residential Property Price Index Statistics
SWE	Residential property prices, long series, NSA	Index 2007=100	1970Q1-2016Q2	— " —	-	BIS Residential Prices Statistics, DBSONline
EA	Residential property prices, new and existing dwellings, whole country, neither SA nor WA (EA19)	Index 1995=100	1980Q1-2016Q2	— " —	-	ECB SDW Residential Property Price Index Statistics

Table A.2: Raw series house prices.

Stock prices						
Country	Description	Original unit	Time-span	Original frequency	(Dis-) aggregation	Source
AUT	VSE WBI index	Index	1970Q1-2016Q2	Quarterly	-	OECD Main Economic Indicators
BEL	All Shares index	— " —	1985Q2-2016Q2	— " —	-	— " —
DEU	CDAX index	— " —	1970Q1-2016Q2	— " —	-	— " —
DNK	KAX CSE All Shares index	— " —	1983Q1-2016Q2	— " —	-	— " —
ESP	IGBM general index	— " —	1985Q1-2016Q2	— " —	-	— " —
FIN	HEX All Share index	— " —	1970Q1-2016Q2	— " —	-	— " —
FRA	Paris Stock Exchange SBF 250 ind	— " —	1970Q1-2016Q2	— " —	-	— " —
GBR	GBR FTSE 100 share price index	— " —	1970Q1-2016Q2	— " —	-	— " —
IRL	ISEQ Overall index	— " —	1970Q4-2016Q2	— " —	-	— " —
ITA	ISE MIB Storico Generale	— " —	1970Q3-2016Q2	— " —	-	— " —
NLD	AEX all shares	— " —	1970Q1-2016Q2	— " —	-	— " —
PRT	BVL general index	— " —	1988Q1-2016Q2	— " —	-	— " —
SWE	AFGX Index	— " —	1970Q1-2016Q2	— " —	-	— " —
EA	Dow Jones EURO STOXX broad	— " —	1987Q1-2016Q2	— " —	-	— " —

Table A.3: Raw series stocks.

10-year government bond yields						
Country	Description	Original unit	Time-span	Original frequency	(Dis-) aggregation	Source
AUT	10y benchmark bond yield	%-points	1970Q1-2016Q2	Quarterly	-	ECB SDW Financial Market Data
BEL	— " —	— " —	— " —	— " —	-	— " —
DEU	— " —	— " —	— " —	— " —	-	— " —
DNK	— " —	— " —	— " —	— " —	-	— " —
ESP	— " —	— " —	— " —	— " —	-	— " —
FIN	— " —	— " —	— " —	Monthly	Simple 3-month average	BoF database
FRA	— " —	— " —	— " —	Quarterly	-	ECB SDW Financial Market Data
GBR	— " —	— " —	— " —	Monthly	Simple 3-month average	BoF database
IRL	— " —	— " —	— " —	Quarterly	-	ECB SDW Financial Market Data
ITA	— " —	— " —	— " —	— " —	-	— " —
NLD	— " —	— " —	— " —	— " —	-	— " —
PRT	— " —	— " —	— " —	— " —	-	— " —
SWE	— " —	— " —	— " —	Monthly	Simple 3-month average	BoF database
EA	— " —	— " —	— " —	— " —	— " —	— " —

Table A.4: Raw series bond yield.

A.5 Random Walk filter

Here we shortly introduce a proxy for optimal band-pass filter called the Random Walk filter. Consider we have an arbitrary discrete time series X_t . A filtered version of X_t , Y_t , is obtained via expression

$$Y_t = B(L)X_t$$

where $B(L)$ is some lag-polynomial. The issue is to find values of $B(L)$ that yield an optimal approximation to the band-pass filter, that is, a filter that extracts those components of X_t with period of oscillations between number of observations p_l and p_u .¹

The optimal band-pass filter $\hat{B}(L)$ would have the form (Cristiano and Fitzgerald, 2003, p. 440)

$$\hat{B}(L) = \sum_{j=-\infty}^{\infty} B_j L^j$$

such that

$$\hat{B}_j = \frac{\sin(jb) - \sin(ja)}{\pi j}, \quad j \geq 1 \quad (\text{A.1})$$

$$\hat{B}_0 = \frac{b - a}{\pi} \quad (\text{A.2})$$

$$a = \frac{2\pi}{p_u}, \quad b = \frac{2\pi}{p_l}$$

Since in practice we don't have infinite amount of data the optimal band-pass filter can clearly never be obtained. Let us denote the hypothetical output from ideal filter as \hat{Y}_t . Now it is our objective to use the actual filter in our disposal, $B(L)$, to obtain data Y_t , and we wish to do it in a manner that we minimize the mean-square error criterion

$$E[(Y_t - \hat{Y}_t)^2 | x], \quad x \equiv [X_1, \dots, X_T]$$

for every time period t . The Random Walk Filter approximation of \hat{Y} is defined as (Cristiano and Fitzgerald, 2003, p. 437)

$$\begin{aligned} Y_t = & B_0 X_t + B_1 X_{t+1} + \dots + B_{T-1-t} X_{T-1} + \tilde{B}_{T-t} X_T \\ & + B_1 X_{t-1} + \dots + B_{t-2} X_2 + \tilde{B}_{t-1} X_1 \end{aligned}$$

¹We have $2 \leq p_l < p_u < \infty$.

where B_j are given as in (A.1) - (A.2). For \tilde{B}_{T-t} we have

$$\tilde{B}_{T-t} = -\frac{1}{2}B_0 - \sum_{j=1}^{T-t-1} B_j \quad t = 3, \dots, T-2$$

and \tilde{B}_{t-1} solves

$$0 = B_0 + B_1 + \dots + B_{T-1-t} + \tilde{B}_{T-t} + B_1 + \dots + B_{t-2} + \tilde{B}_{t-1}$$

Using the Random Walk filter code provided by original authors is rather simple: We feed our unfiltered stress index ψ to algorithm $B^{RW}(p_l, p_u)$ with inputs p_l and p_u corresponding to values indicating periodicity band endpoints in given time unit. The code for the algorithm is available at the homepage of Federal Reserve Atlanta under address <https://www.frbatlanta.org/cqer/research/bpf.aspx>.

A.6 Matlab code for Blacmman-Tukey spectral density estimator

```
function [crossSpectrum,frequencies] =...
    crossSpectrumEstimateBT(...
        series1,....
        series2,...
        L,...
        type,...
        nfft...
    )

%%%%%%%%%%%%%%%%%%%%%%%%%%%%%%%%%%%%%%%%%%%%%%%%%%%%%%%%%%%%%%%%%%%%%%%%
%                               crossSpectrumEstimateBT.m
%%%%%%%%%%%%%%%%%%%%%%%%%%%%%%%%%%%%%%%%%%%%%%%%%%%%%%%%%%%%%%%%%%%%%%%%

% Spectral density estimation as explained in Voutilainen(2017).
% This function takes in two real-valued series and produces an estimate
% for their cross-spectrum. The method used is the so-called Blackman-Tukey
% method which estimates the spectral density through cross-covariances.
%
% COMMUNICATES WITH:
```

```

%      - Econometrics toolbox
%
% INPUTS :
%   - series1: vector of values representing input series 1
%   - series2: vector of values representing input series 2
%   - L: integer representing lag-window length
%   - type: string representing whether we want cross-spectrum estimate
%           (smoothed periodogram) or the "raw" periodogram
%   - length of FFT (optional)
%
% OUTPUT:
%   - crossSpectrum: vector of values corresponding to 1-sided
%                   cross-spectral estimate
%   - frequency interval corresponding to crossSpectrum
%
% REFERENCES:
%   - Priestley(1981): Spectral Analysis and Time Series Vol. 1 and 2
%   - Voutilainen(2017): Frequency-domain View on Financial Cycles:
%                       Empirical Evidence from Europe, MSc thesis
%                       Goethe Universität Frankfurt
%   - http://blogs.uoregon.edu/seis/wiki/unpacking-the-matlab-fft/
%   - http://dsp.stackexchange.com/questions/34642/practical-cross-spectrum-estimation-using-blackman-tukey-approach
%
% OPTIONS
%   - type = 'spectrum': Cross-spectrum estimate
%   - type = 'periodogram': Periodogram estimate
%
%%%%%%%%%%%%%%%%%%%%%%%%%%%%%%%%%%%%%%%%%%%%%%%%%%%%%%%%%%%%%%%%%%%%%%%%
% Copyright:
%       Ville Voutilainen
%       Bank of Finland
%       Edited: September 2016
%%%%%%%%%%%%%%%%%%%%%%%%%%%%%%%%%%%%%%%%%%%%%%%%%%%%%%%%%%%%%%%%%%%%%%%%

```

Input Checks

```

if length(series1) ~= length(series2)

```

```

errorldg( ['Error in crossSpectrumEstimateBT; Lengths of input '....
          'series do not match!'], 'Well this is awkward... ');
error(['Error in crossSpectrumEstimateWelch; Lengths of input' ...
      'series do not match!'])
end

if strcmp(type, 'spectrum') == 1 || strcmp(type, 'periodogram') == 1
    % all ok
else
    errorldg( ['Error in crossSpectrumEstimateBT; Invalid '....
              '"type input string"!'], 'Well this is awkward... ');
    error(['Error in crossSpectrumEstimateWelch; Invalid' ...
          '"type input string"!'])
end

```

Parameter values

```

% Length of total sample
N = length(series1); % Only for series 1 since both have equal length

% If user has not defined length of FFT, set it as in eq. 9.5.7 of
% Priestley(1981).
% Make sure that nfft is ODD, if not then pad the series with
% a zero.
if nargin < 5 % no nfft set
    nfft = 2*(N-1) + 1;
    if rem(nfft,2) == 0
        nfft = nfft + 1;
    end
else % nfft set
    if rem(nfft,2) == 0
        nfft = nfft + 1;
    end
end

end

% Total length of the lag-window, must be ODD
L = 2.*round((L+1)/2)-1;

```

```
% Truncation parameter for the lag-window
M = (L-1)/2;
```

```
% Sampling frequency
fs = 1;
```

Cross-covariances

```
% Cross-correlation using crosscov, N-1 lags
crossCorrelation = crosscorr(series1,series2,N-1);
```

```
% Convert into cross-covariance
crossCovariance = crossCorrelation * std(series1) * std(series2);
```

Apply lag window if necessary

```
if strcmp(type,'spectrum') == 1
    % Define lag-window
    win = parzenLagWindow(L);

    % Window cross-covariances
    xw = zeros( 2*(N-1) + 1 ,1);
    counter1 = 0;
    counter2 = 0;
    for s = -(N-1) : N-1
        counter1 = counter1 + 1;
        if abs(s) <= M
            counter2 = counter2 + 1;
            xw(counter1,1) = win(counter2,1) * crossCovariance(counter1,1);
        end
    end
else
    xw = crossCovariance;
end
```

Get frequency interval

```
% 1-sided frequency intervals (nfft odd, positive Nyquist frequency drops)
```

```

Nyg = fs/2;
df = fs/nfft;
freq2Sided = (0:(nfft-1))*df;
freq2Sided(freq2Sided>Nyg) = freq2Sided(freq2Sided>Nyg)-(Nyg*2);
freq2Sided = freq2Sided';
freq1Sided = freq2Sided(1:(nfft-1)/2 + 1);
angularFreq1Sided = 2*pi*freq1Sided;

```

Estimation of the cross-spectrum from cross-covariances

```

% In order to calculate this expression in practical terms, we need to
% circularly shift the input vector for fft. Also, in order to obtain
% smoother estimation, we want to use user-provided nfft value in the fft.
% Thus, depending on the value nfft, we might need to to zero-pad vector xw.
% We cannot let fft function do this since it will break the symmetry.
% Therefore, this is done manually.

```

```

% Since nfft and length(xw) are both odd, twoTimesZeros must be even
twoTimesZeros = nfft - length(xw);

```

```

% Shift the vector xw circularly to match DFT input and pad the zeros in
% between in order to preserve symmetry in fft

```

```

xw = [ xw((N-1)+1 : end,1);...
       zeros(twoTimesZeros/2,1);...
       zeros(twoTimesZeros/2,1);...
       xw(1:N-1,1)  ];

```

```

% DFT of circularly shifted and zero padded windowed cross-correlations,
% see equation 3.8 of Voutilainen(2017). DFT calculated as in equation
% 2.15 of Voutilainen(2017).

```

```

P2Sided = 1/length(xw) * fft(xw) ;

```

```

% Since input series are inherently real-valued, it is enough to obtain
% only one-sided cross-spectrum. Since nfft is ODD, we have NEITHER of the
% Nyquist frequency values in the middle of the vector, only values that
% are df/2 smaller than Nyquist frequency value. Also, there is no zero
% frequency value for negative frequencies

```

```
P1Sided = P2Sided(1:(nfft-1)/2 + 1 );

% If we deal with autospectrum, the sine terms appearing in eq 6.2.54
% should cancel and we are reduced to equation 6.2.51. However, the FFT
% above still gives tiny imaginary terms for autospectrum as well due to
% numerical inaccuracies. Here we force these value real.
if series1 == series2
    P1Sided = real(P1Sided);
end

% Since both positive and negative halves of the frequency
% range display half of the energy of the signal, multiply all
% observations in the one-sided estimate by two, EXPECT values at zero
% frequency (no Nyquist frequency value present, thus only frequency zero
% value is not multiplied!)
P1Sided(2:end) = 2* P1Sided(2:end);
```

Output

```
crossSpectrum = P1Sided;
frequencies = angularFreq1Sided;
```

```
end
```

A.7 Power Cohesions

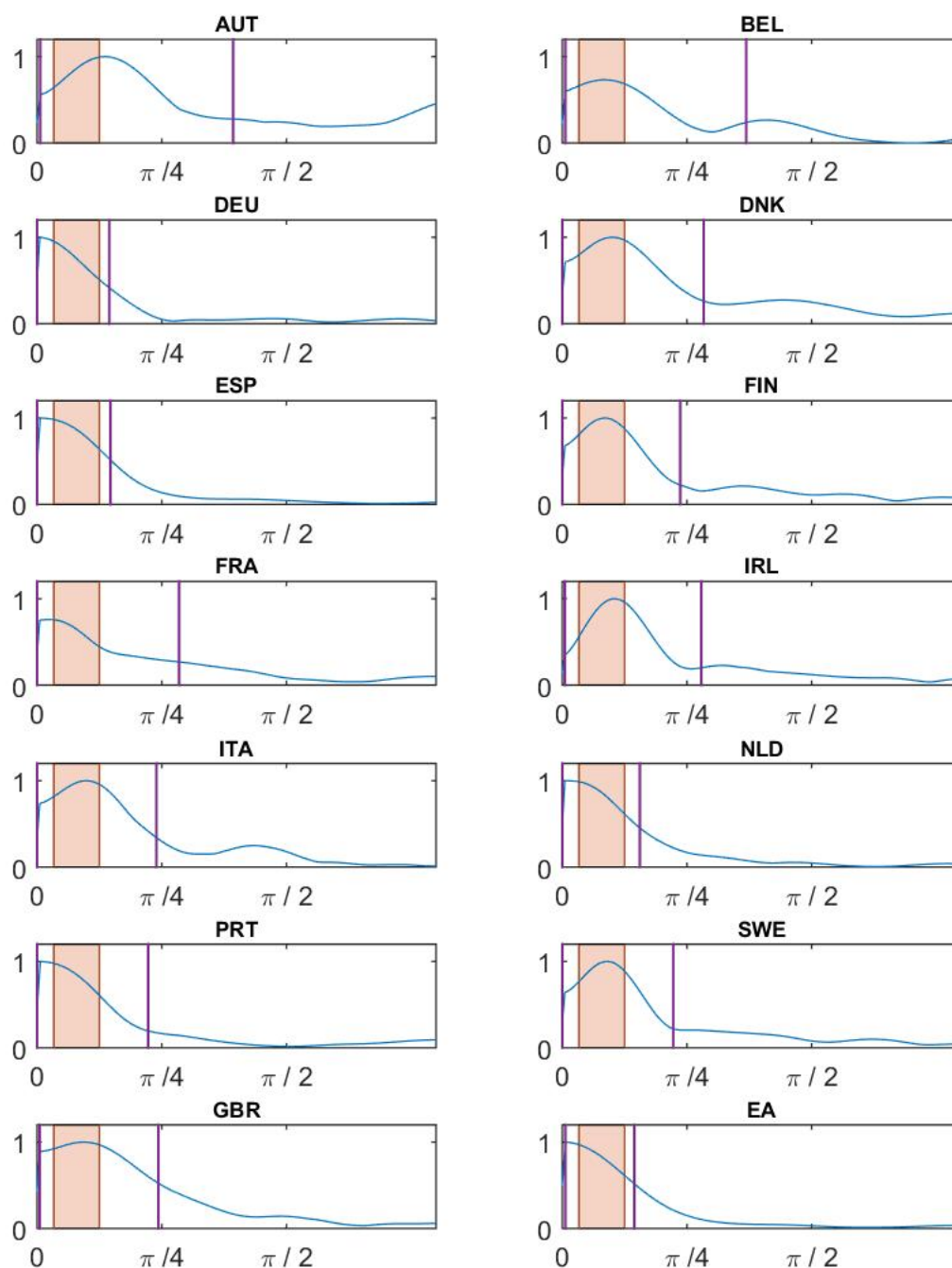


Figure A.1: Power Cohesions for individual countries. x-axis depicts angular frequency interval $[0, \pi]$, and y-axis depicts PCoh value normalized to unit interval. Angular frequencies are converted to corresponding time periods via formula $\omega = 2\pi\frac{1}{T}$, where T is the period length in quarters. Shaded regions represent period interval 8-30 years. Purple vertical lines correspond to identified frequency band endpoints.

A.8 Crisis Database

Table A.5 describes the crisis periods compiled by Laeven and Valencia (2012) for each of the countries used in this thesis, except for the euro area aggregate as the currency union as a whole is not included in the dataset. The aim of the dataset is to capture banking crises of systemic nature. In order for a period to be considered as one with banking crisis, two conditions have to be met. First, country must exhibit significant signs of financial distress, indicated e.g. by bank runs, bank liquidations etc. Second, financial distress resulted in notable banking policy interventions. In the original paper starting/ending periods of crises are sometimes given at monthly, sometimes at yearly accuracy. In the case starting/ending period is only given at yearly accuracy we set the start/end to Q1/Q4 of corresponding year.

Country	Period(s)
AUT	2008Q3-2010Q4
BEL	2008Q3-2010Q4
DEU	2008Q3-2010Q4
DNK	2008Q3-2010Q4
ESP	1977Q1-1981Q4, 2008Q3-2010Q4
FIN	1991Q3-1995Q4
FRA	2008Q3-2010Q4
IRL	2008Q3-2010Q4
ITA	2008Q3-2010Q4
NLD	2008Q3-2010Q4
PRT	2008Q3-2010Q4
SWE	1991Q3-1995Q4, 2008Q3-2010Q4
GBR	2007Q3-2010Q4

Table A.5: Crisis periods for the sample countries in Laeven and Valencia (2012) banking crisis data set.

Bibliography

- Aikman, David; Andrew Haldane, and Benjamin Nelson (2015). “Curbing the credit cycle”. In: *The Economic Journal* vol. 125, pp. 1072–1109.
- Alessi, Lucia and Carsten Detken (2011). “Quasi real time early warning indicators for costly asset price boom/bust cycles: A role for global liquidity”. In: *European Journal of Political Economy*, no. 27, pp. 520–533.
- (2014). “On policymakers’ loss functions and the evaluation of early warning systems: Comment”. In: *Economics Letters*, pp. 338–340.
- Babecký, Jan et al. (2012). “Banking, Debt, and Currency Crises - Early Warning Indicators for Developed Countries”. In: *ECP Working Paper Series*, no. 1485.
- Bartlett, Maurice (1948). “Smoothing periodograms for time series with continuous spectra”. In: *Nature* vol. 16, pp. 686–687.
- Behn, Markus et al. (2013). “Setting Countercyclical Capital Buffers based on Early Warning Models - Would It Work?” In: *ECB Working Paper Series*, no. 1604.
- Blackman, Ralph and John Tukey (1958). *The Measurement of Power Spectra. From the Point of View of Communications Engineering*. Dover Publications Inc.
- Borio, Claudio (2014). “The financial cycle and macroeconomics: What have we learnt?” In: *Journal of Banking and Finance* vol. 45, pp. 182–198.
- Bussière, M and M Fratzschem (2006). “Towards a new early warning system of financial crises”. In: *Journal of International Money and Finance* vol. 25, no. 6, pp. 953–973.
- Cajori, Florian (1894). *A History of Mathematics*. MacMillan and Co./ Google Book Search.
- Claessens, Stijn; Ahyan Kose, and Marco Terrones (2011). “Financial Cycles: What? How? When?” In: *IMF Working Papers*, no. 76.
- Cristiano, Lawrence and Terry Fitzgerald (2003). “The Band Pass Filter”. In: *International Economic Review* vol. 44, no. 2, pp. 182–198.
- Demirgüç-Kunt, Asli and Enrica Detragiache (2000). “Monitoring Banking Sector Fragility: A Multivariate Logit Approach”. In: *The World Bank Economic Review* vol. 14, no. 2, pp. 287–307.

- Detken, Carsten et al. (2014). “Operationalizing the countercyclical capital buffer: indicator selection, threshold identification and calibration options”. In: *ESRB Occasional Paper Series*, no. 5.
- Dominguez, Alejandro (2016). *Highlights in the History of the Fourier Transform*. URL: <http://pulse.embs.org/january-2016/highlights-in-the-history-of-the-fourier-transform/>.
- Drehmann, Mathias; Claudio Borio, and Kostas Tsatsaronis (2012). “Characterizing the financial cycle: don’t lose sight of the medium term!” In: *BIS Working Papers* vol. 44, no. 380, pp. 182–198.
- dsprelated.com (2017). *Mathematics of the DFT - Shift Theorem*, accessed 13.2.2017. URL: https://www.dsprelated.com/freebooks/mdft/Shift_Theorem.html.
- Frankel, Jeffrey and Andrew Rose (1996). “Currency crashes in emerging markets: An empirical treatment”. In: *Journal of International Economics* vol. 41, pp. 351–366.
- Geanakolpos, John (2010). “The Leverage Cycle”. In: *NBER Macroeconomics Annual 2009*.
- Holló, Dániel; Manfred Kremer, and Marco Lo Duca (2012). “CISS - A Composite Indicator of Systemic Stress in the financial system”. In: *ECP Working Paper Series*, no. 1426, pp. 182–198.
- Huotari, Jarkko (2015). “Measuring financial stress - A country specific stress index for Finland”. In: *Bank of Finland Discussion Papers*, no. 7.
- Laeven, Luc and Fabián Valencia (2012). “Systemic Banking Crises Database: An Update”. In: *IMF Working Paper Series*, no. 12/163.
- Lo Duca, Marco and Tuomas Peltonen (2013). “Assessing systemic risks and predicting systemic events”. In: *Journal of Banking and Finance* vol. 37, pp. 2183–2195.
- Mathworks (2017). *Fast Fourier transform*, accessed 24.2.2017. URL: <https://www.mathworks.com/help/matlab/ref/fft.html>.
- Oppenheim, Alan (2017). *Discrete-Time Fourier Series - MIT Open Courseware*, accessed 2.1.2017. URL: https://ocw.mit.edu/resources/res-6-007-signals-and-systems-spring-2011/lecture-notes/MITRES_6_007S11_lec10.pdf.
- Priestley, M.B. (1981a). *Spectral Analysis and Time Series Vol 1: Univariate Series*. 1st. Academic Press.
- (1981b). *Spectral Analysis and Time Series Vol 2: Multivariate Series, Prediction, and Control*. 1st. Academic Press.
- Sarlin, Peter (2013). “On policymakers’ loss functions and the evaluation of early warning systems”. In: *Economics Letters*, pp. 1–7.

- Schularick, Moritz and Alan Taylor (2012). “Credit booms gone bust: Monetary policy, leverage cycles, and financial crises, 1870-2008”. In: *American Economic Review* vol. 102, pp. 1029–1061.
- Schüler, Yves; Paul Hiebert, and Tuomas Peltonen (2015). “Characterizing the financial cycle: a multivariate and time-varying approach”. In: *ECB Working Paper Series*, no. 1846.
- Selesnick, Ivan (2017). *Properties of the DFT - NYU Lecture Notes EL 713: Digital Signal Processing II*. URL: <http://eeweb.poly.edu/iselesni/EL713/zoom/dftprop.pdf>.
- stackexchange.com (2017). *Practical cross-spectrum estimation using Blackman-Tukey approach, accessed 13.2.2017*. URL: <http://dsp.stackexchange.com/questions/34642/practical-cross-spectrum-estimation-using-blackman-tukey-approach/>.
- Stoica, Petre and Randolph Moses (2004). *Spectral Analysis of Signals*. Prentice Hall.
- Töölö, Eero; Helinä Laakkonen, and Simo Kalatie (2017). “Evaluating indicators for use in setting the countercyclical capital buffer”. In: *The International Journal of Central Banking, forthcoming*.
- Welch, Peter (1967). “The Use of Fast Fourier Transform for the Estimation of Power Spectra: A Method Based on Time Averaging Over Short, Modified Periodograms”. In: *IEEE Transactions on Audio and Electroacoustics* vol. 15, no. 2, pp. 70–73.
- WolframMathWorld (2017). *Fourier Transform, accessed 5.3.2017*. URL: <http://mathworld.wolfram.com/FourierTransform.html>.

I have written the present thesis myself and have used exclusively the sources and aides mentioned. This thesis has not yet been submitted as an examination in another degree programme. All passages taken word-by-word or the meaning of which are quoted from published or unpublished texts, as well as all indication based on oral accounts, have been marked as such.

Ville Voutilainen